

**Figure 3-15: Core WHG-12 (0–60 cm).** (Format: 8bit tiff inverted; export:256 greyscale, scale 400%, png).

### 3.4 Long-term average catchment sediment yield

The long-term average specific sediment yield from catchments draining to the upper harbour (i.e., west of Limestone Island) was estimated from the quantity of sediments deposited in major depositional habitats (i.e., mangrove, saltmarsh, un-vegetated intertidal flat) over the last 50 years (section 2.4). Although there are uncertainties in the estimate of catchment sediment-yield estimate, the method has the significant advantage that it is largely based on measured long-term sediment accumulation rates and sediment bulk density. The estimate is also likely to be conservative given that a proportion of the catchment sediment delivered to the upper harbour has been exported to the lower harbour (section 4).

The average specific sediment yield ( $S_y$ ) from the  $\sim 220 \text{ km}^2$  upper-harbour catchment is estimated as  $138 \pm 28 \text{ t/km}^2/\text{yr}$  (95% Confidence Interval) over the last 50 years. This estimate is within the range of values estimated for the major sub-catchments using NIWA's WRENZ model:  $122 \text{ t/km}^2/\text{yr}$  (Hātea),  $355 \text{ t/km}^2/\text{yr}$  (Otaika) and  $60 \text{ t/km}^2/\text{yr}$  (Mangapai).

### 3.5 Contemporary sediment sources

#### 3.5.1 Harbour

Assessment of the contemporary sources of sediment accumulating in the harbour was determined by sub-catchment (inflows) and land-use type. Inflow sources were assessed using surficial sediment samples collected from the river deltas at sub-catchment outlets. These included the Hātea River, Otaika River, Mangapai River and a sample from Calliope Bay, which represents coastal sediment that can be carried in and out of the harbour. The results of the sediment-source analysis provided by the IsoSource modelling are plotted as maps showing the predicted percentage contribution of the major sub-catchment sources (Figs 3-16 to 3-19). Blacksmith Creek was also modelled as indicative of the inflows to the outer harbour but was not included in the contour plots. Appendix B presents the stable-isotope and percent carbon data used to model the isotopic and soil proportions for each sediment source.

Note that at almost all sampling locations in the harbour, the top-most 2 cm surface sediment layer coincides with the SML determined by the <sup>7</sup>Be data (Table 3-1) which implies the CSSI samples are integrating the source soils being mixed in that layer. Based on the SAR data (Table 3-1), that integration is likely to encompass from 3 to 6+ years sedimentation and therefore is representative of the soil sources contributing to that location.

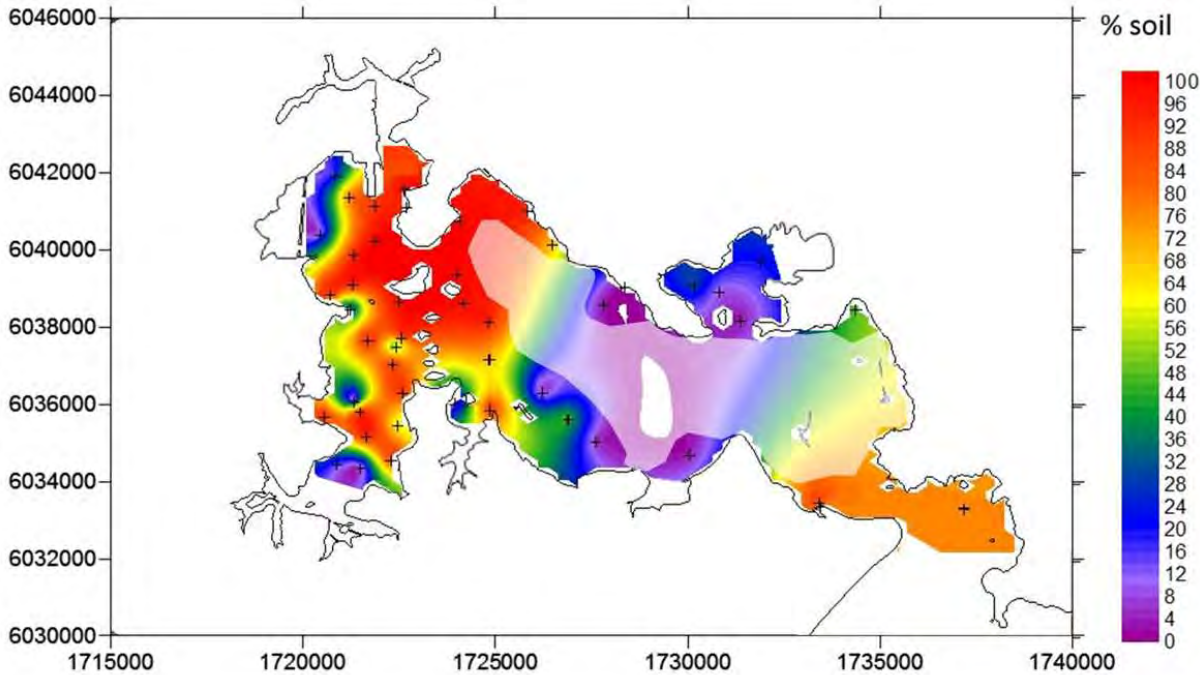


**Figure 3-16: Proportion of Hātea sub-catchment soils in harbour sediments.** The fogged area covers indicative extrapolated areas with no data support. Map co-ordinate system: NZTM2000.

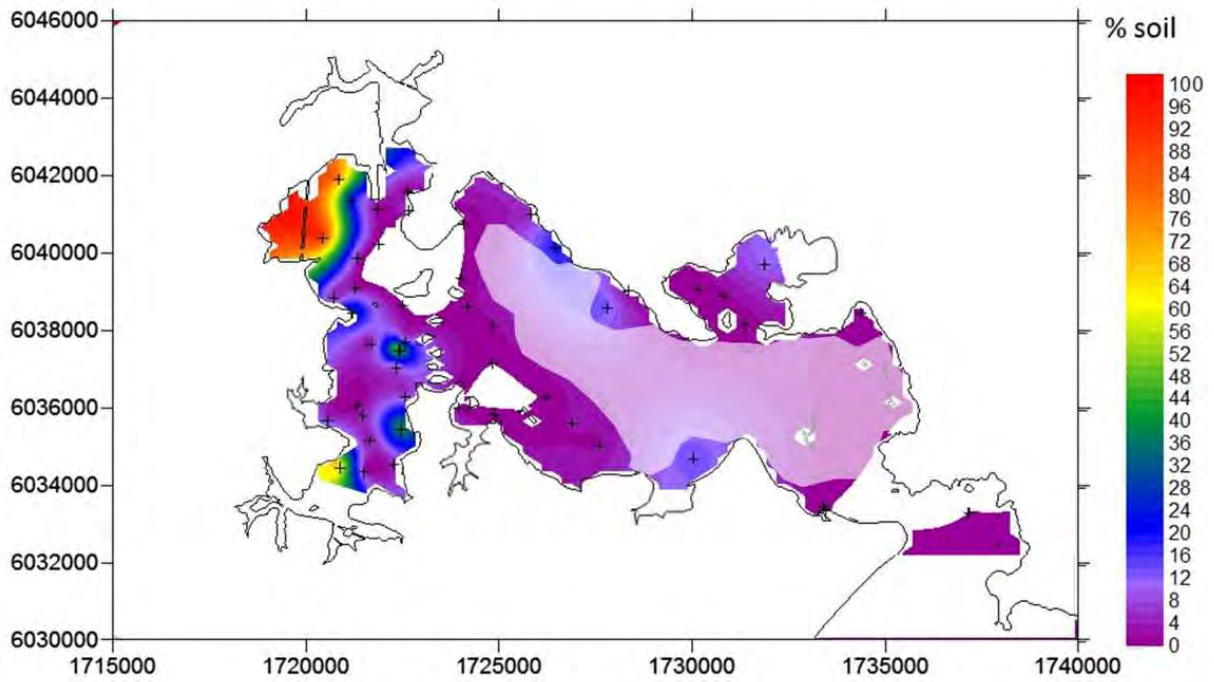


**Figure 3-17: Proportion of Otaika sub-catchment soils in harbour sediments.** The fogged area covers indicative extrapolated areas with no data support. Map co-ordinate system: NZTM2000.

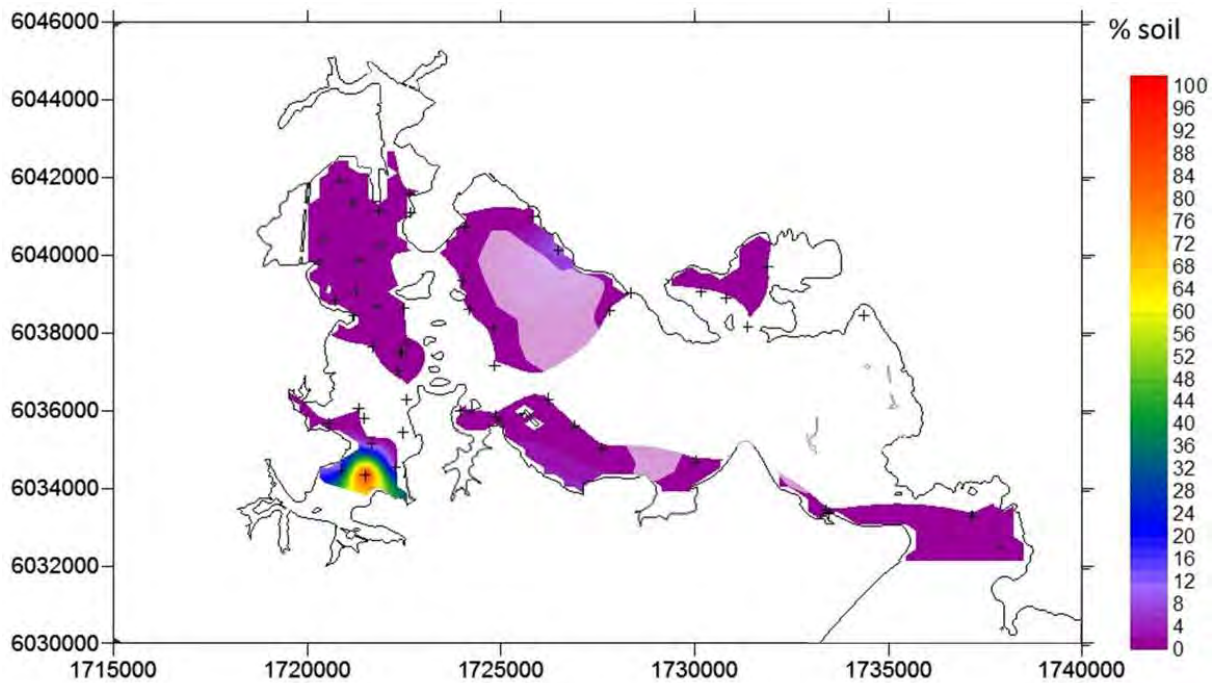


**Figure 3-18: Proportion of Mangapai sub-catchment soils in harbour sediments.** The fogged area covers indicative extrapolated areas with no data support. Map co-ordinate system: NZTM2000.

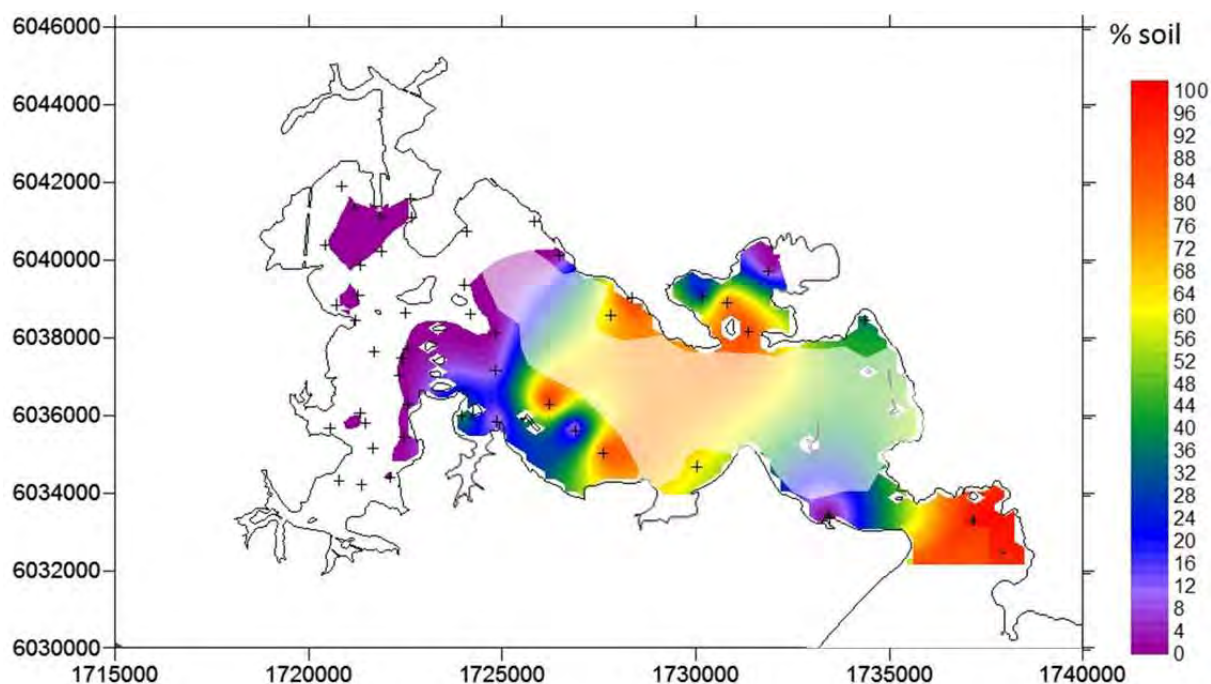


**Figure 3-19: Proportion of Calliope Bay coastal sediments in the harbour sediments.** The fogged area covers indicative extrapolated areas with no data support. Map co-ordinate system: NZTM2000.

Although no flow data was used to produce these spatial distribution patterns, the distribution pattern of sediment from the Otaika River (Figure 3-17) is consistent with the predicted sediment accumulation pattern from the hydrodynamic model (Figure 3-1 to Figure 3-3) lending credibility to these results.

The CSSI modelling also showed that the inner harbour sediments were also influenced by the Portland cement plant loading wharf (Figure 3-20). The Portland isotopic signature was taken from the surface sediment layer of core WHG-2 and was detected at low levels throughout much of the harbour. However, areas affected by elevated proportions of this sediment tended to have raised levels of uncertainty with  $n$  values exceeding 300. This indicates that “Portland sediment” is probably a proportion of historical sediment which has been mixed up into the SML rather than a recent deposition event. The mechanism for the upwards movement of the historical sediment could be associated with bioturbation and excavation of the numerous crab burrows in the upper harbour. Burrows of the mud crab, *Austrohelice crassa*, can extend to depths of >30 cm (e.g., Needham et al. 2012).

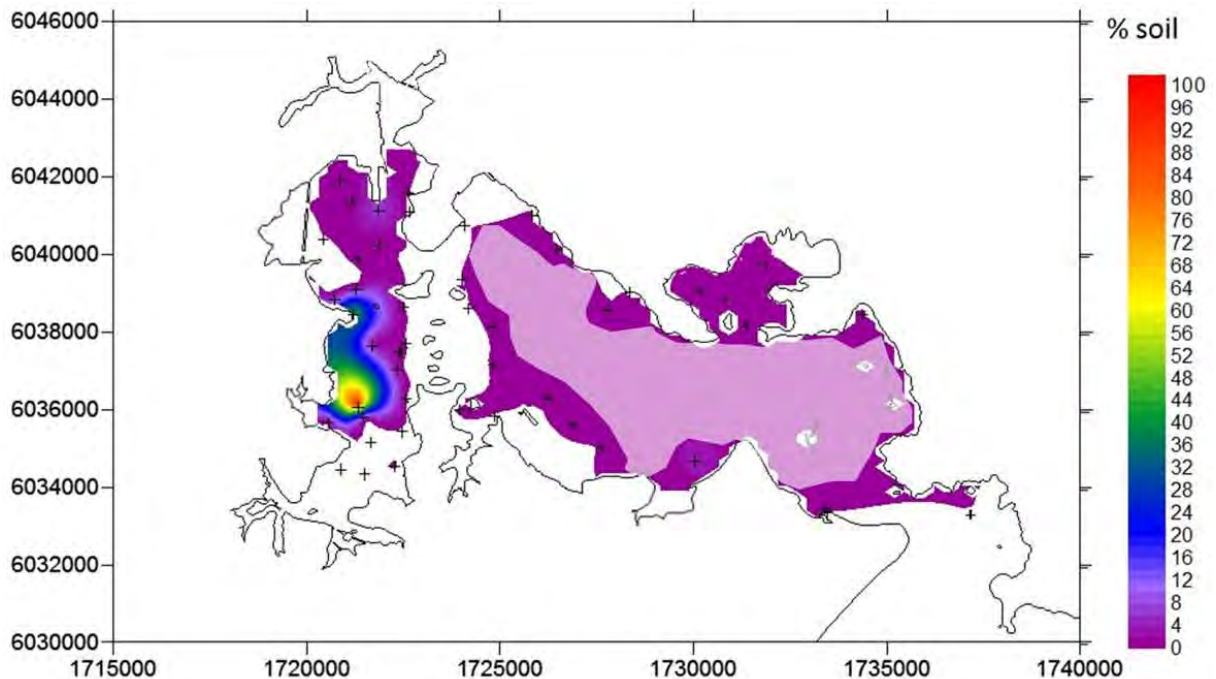


**Figure 3-20: Proportion of Portland sediments in the harbour sediments.** The fogged area covers indicative extrapolated areas with no data support. Map co-ordinate system: NZTM2000.

The analysis and spatial modelling of the potential sources of present-day harbour sediments indicates that terrigenous sediments derived from the Hātea River inflow are the most widely dispersed and accumulating in the upper and middle-reaches of Whangarei Harbour. Sediments derived from Otaika and the Mangapai sub-catchments as well as the Portland sediments are locally accumulating in the harbour near these river outlets. Present-day sedimentation in the lower reaches of the harbour is dominated by coastal sediments, most likely transported into the harbour by tidal currents. The spatial variability in the sources of harbour sediments indicates that there has been much reworking of these sediments within the harbour.

### 3.5.2 Catchment

Evaluation of the three river inflows used each river delta sample as the mixture and estimated the contribution of soil/sediment in that mixture from the tributaries and land use in the upstream catchment.

#### Hātea River

As previously noted (2.4.4 Isotopic disconnect), there was a significant difference in the CSSI signatures in the Hātea River delta sediment sample and the sediment in the Hātea River at Mair Park from the upstream catchment. Because of this, the Hātea River was assessed as upper and lower sections, the separation being at Mair Park (Figure 3-21).

Detailed assessment of the upper Hātea River found that almost all (>90%) of the recent sediment in the Hātea River at Mair Park came from the catchment upstream of Tikipunga (subcatchment A, Figure 3-21) with <10% coming from the Otangarei Stream system (subcatchment B) and the steep forest land on the eastern side of the river (subcatchment D). That sediment comprised 23.6 % (SD 8.1) pine forest, 10.9 % (SD 2.2) pasture of all

types, 6.6 % (SD 3.9) pasture sub soil and 58.9 % (SD 5.5) of native forest including totara. This native forest soil would include recent land clearance and slips.

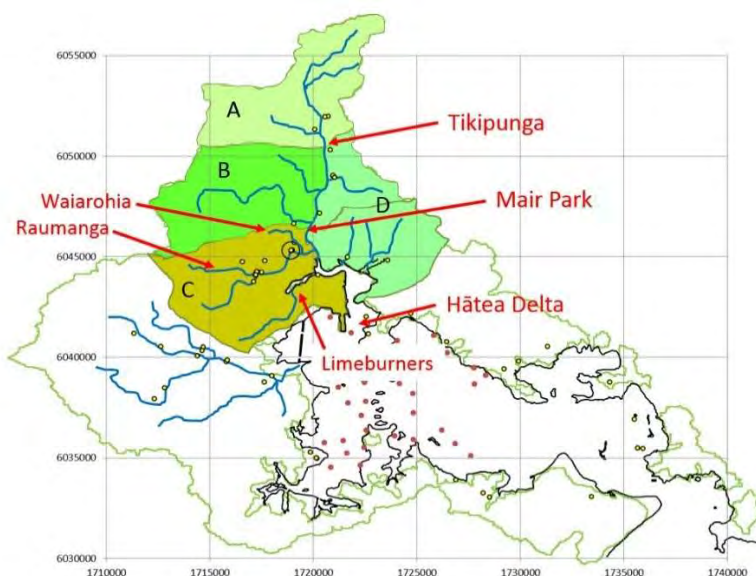


**Figure 3-21: Hātea River catchment divided into subcatchments.** Subcatchments are assigned letters for convenience of discussion in the text.

Assessment of the sediment sources to the Hātea River Delta site considered the upper Hātea River at Mair Park, the Raumanga Stream system, Limeburners Creek, Waioneone Creek and the Awaroa Creek. These results showed that a maximum of 9 % (SD 3.3) of the sediment in the delta came from the upper Hātea River, the Awaroa and Waioneone Creeks contributed up to 3 % (SD 1.2), Limeburners Creek contributed up to 31 % (SD 4.8) and the Raumanga Stream system contributed up to 56 % (SD 6.5). The disproportionately low proportion of upper Hātea River sediment in the river delta sample may be due to the thickness of the sediment layer sampled and the lack of recent sediment deposition due to low rainfall conditions prior to sampling. The low level of the Hātea River and lack of sediment deposits in the stony river bed was noted at all sites upstream of Mair Park.

Deconstruction of the Raumanga Stream system showed that most (90 %; SD 3.4) of the sediment from this stream were sub-soils presumably from bank erosion and slips in the Maunu Road tributary, which potentially includes the Waiairohia Stream although the latter was not sampled. The main Raumanga Stream contributed up to 5 % (SD 2.9) as subsoil with up to 4 % (SD 1.6) native forest including totara. Pasture signature was present but at <1 %.

Deconstruction of the Limeburners Creek sediment source showed that up to 90% was subsoil of the type found along the Maunu Road tributary (45 %; SD 2.6) and the main Raumanga Stream (44 %; SD 2.1) with up to 10 % (SD 1.2) as native forest including Totara. Although there is no direct connection between Limeburners Creek and the Raumanga Stream system, a major tributary of the Raumanga Stream, the Waiponamu Stream, shares the hill catchment with the Te Waiiti Stream that flows into Limeburners Creek. This suggests that the subsoils from that area of the catchment are similar for both streams.

## Otaika River

The Otaika River delta receives sediment from the main Otaika River system (80 %; SD 3.5) and the Puwera Stream system (20 %; SD 2.5) (Figure 3-22). Deconstruction of the Otaika River sediment shows that above the confluence with the Puwera Stream, 65% of the sediment comes from the upper catchment including the Otakaranga Stream catchment and the Otaika Valley streams. The rest of the sediment comes from pasture (25.4 %; SD 1.6) and native forest (7.6 %; SD 3.1) on steeper northern hills.

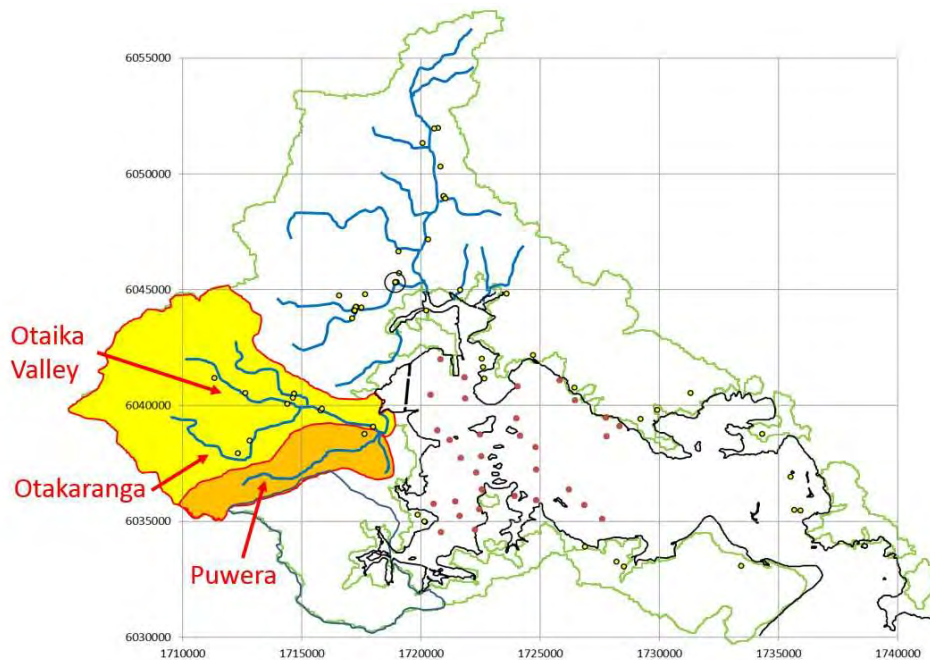


**Figure 3-22: Otaika River system showing the main subcatchments and tributaries.**

The Otaika Valley river catchment above the confluence with the Otakaranga Stream produces 11.5 % (SD 0.6) of the upper catchment sediment, mostly from pasture with an underlying native forest (totara) signature. The Otakaranga Stream catchment contributes 86 % (SD 4.8) of the sediment with a further 2.5 % (SD 5.1) from the northern tributary. Deconstruction of the Otakaranga Stream sediment shows that 11 % (SD 2.1) comes directly from pasture, 19 % (SD 1.5) comes from bank erosion similar to that on Tavinor Road and 69 % (SD 1.5) is from native forest soils. As there are few large areas of native forest in this subcatchment, this is probably from newly established pasture on recently cleared forest land. A suggestion by NRC (Ben Tait, pers. comm.) that the land in this subcatchment has been converted from pine forest into pasture is a reasonable explanation but implies that the soil reference samples used in the CSSI technique were missing a pine subsoil sample and the native soil was closest.

Deconstruction of the Puwera Stream sediment sources showed that 94 % (SD 2.3) were from subsoils which may have been bank erosion or recent slips. There was a small proportion of pine (4.4 %, SD 3.2) and traces of pasture and native forest soils present.

## Mangapai River

Sediment in the Mangapai River delta was taken from the surface of core WHG-1 and may be affected by relocation of material around the inner harbour. Assuming that the main supply of sediment in the delta was from terrigenous sources, the sediment composition was deconstructed using the land-use soil types. The results indicate that around 75 % (SD 1.9) of the sediment was from bank erosion type material which includes dirt roads and road cuttings. The rest of the sediment came from exotic pine forestry 10% (SD 2.3), pasture 7 % (SD 1.8) and native forest 7.5 % (SD 1.2).

## Summary

On a *pro rata* basis, these results can be converted to give a best estimate of the four main soil land-use types discharged into the upper harbour from the three river inflows (Figure 3-23). The subsoil component includes bank erosion and native forest component includes totara. There is high uncertainty on the proportions of soil from the Hātea River because of the isotopic disconnect in the lower Hātea River.

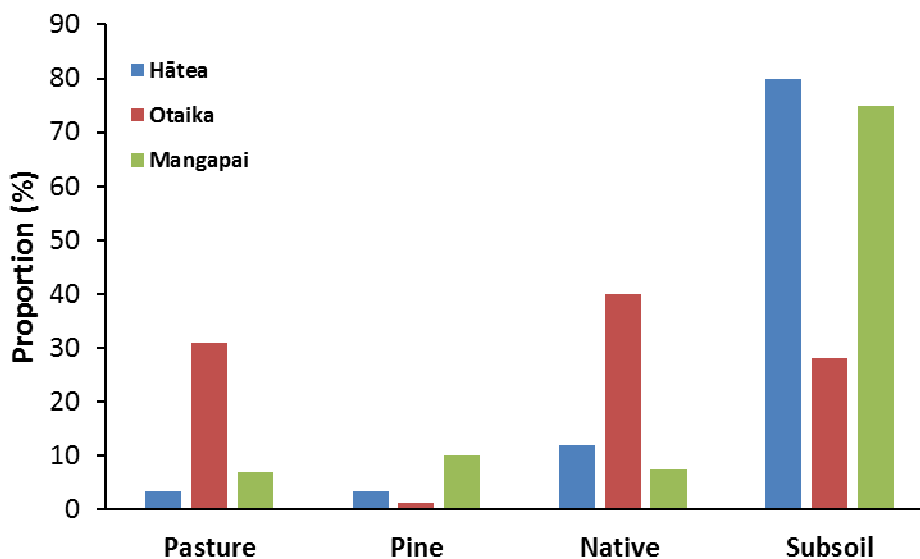


Figure 3-23: Summary of the proportions of landuse soils discharged from the three main inflows.

## 4 Synthesis

In this section we integrate information collected as part of this study with other sources of information to: (1) reconstruct where catchment-derived sediments are accumulating in Whangarei Harbour; (2) identify the major sources of these sediments; and (3) consider these changes in the wider context of historical environmental changes in other North Island estuaries.

### 4.1 Recent sedimentation history of Whangarei Harbour

The recent sedimentation history of Whangarei Harbour is reconstructed based on information derived from the dated sediment cores, analysis of contemporary sediment sources and sediment-transport modelling. This interpretation is supplemented by information gathered from relevant previous studies and historical information. Figure 4-1 summarises spatial patterns of recent sedimentation history of Whangarei Harbour.

The  $^{210}\text{Pb}$  dating and x-ray images of the sediment cores provide information on sediment accumulation rates SAR and qualitative information on the types of sediment that have accumulated in the harbour over the last ~150 years. These data indicate that: (1) the upper harbour has substantially infilled with catchment muds and fine sands; and that (2) the muds in particular have been exported from the upper harbour to the lower harbour where they are preferentially accumulating in the bays and inlets that indent the northern shoreline (Fig. 4-1).

In the Mangapai arm, apparent declines in SAR during the early- to mid-20<sup>th</sup> century are most likely due to reduced sediment delivery associated with a reduction in tidal inundation as the intertidal flats have vertically accreted over time. There is poor agreement between the  $^{210}\text{Pb}$  and  $^{137}\text{Cs}$  dating at site WHG-3 so that the high apparent  $^{210}\text{Pb}$  SAR of 9.4 mm/yr may not be reliable. In the Hātea arm, muds are also accumulating on intertidal flats (i.e., sites WHG-6, WHG-14) north of the main channel entering the upper harbour between the Onerahi peninsula and Limestone Island. Radioisotope data from cores WHG-4 and WHG-5 show that long-term mud accumulation is not occurring on the intertidal flats west of Limestone Island, which are exposed to the 5 km+ east–west fetch.



**Figure 4-1: Summary of recent sedimentation in Whangarei harbour. Information sources: present study and Millar (1980).** Mud sinks: (1) Northern shore from Onerahi east to Jackson's Bay (east end of mud sink-1), long-term mud accumulation sub-tidally but likely to be reworked on the intertidal flats by waves; (2) long-term mud accumulation in sub-tidal habitats, Parua Bay and Munro Bay.

The export of fine sediments to the lower harbour as the upper harbour has progressively infilled is consistent with the sediment-core record from the intertidal flats. As the intertidal volume shrinks due to sedimentation, the accommodation space for future sediment deposition is reduced. Water depth also decreases and short-period waves characteristic of fetch-limited estuaries become increasingly effective at resuspending muds. This is because the orbital motions under these waves are rapidly attenuated in the water column and typically only become competent at reworking bed sediments in water depths of less than 1-2 metres, largely depending on wave period (Green et al. 1997, Swales et al. 2004). Loss of sediment accommodation space also occurred in the tidal reach of the Hātea River due to reclamations associated with the development of the Port of Whangarei since the early 1900s. Much of this reclamation work has occurred since the early 1950s (Northland Regional Council 1989). The hydrodynamics of the Hātea arm of the upper harbour, in particular, would also have been modified to some extent by reclamation. However, this reclamation is likely to have been a secondary factor, with the progressive infilling of the entire upper estuary driving fine-sediment export to the lower estuary.

In Parua Bay, core WHG-11 also indicates rapid vertical accretion of the intertidal flats until the early 1950s when SAR reduced, mostly likely as a result of reduced tidal inundation rather than sediment supply. Today, the intertidal flat is accumulating sediment (2.9 mm/yr)

at a similar rate to the central sub-tidal basin (WHG-10, 2.2 mm/yr). Parua Bay has a small catchment so that a substantial fraction of the sediment accumulating in this basin has been derived from sources other than Parua Bay catchment. Sediment-transport modelling undertaken in the present study indicates that some of the mud discharged with stormwater from the Hātea and Otaika rivers is exported to lower harbour and deposits in the bays indenting the northern shoreline of the lower harbour. This pattern of mud deposition is also consistent with Millar's (1980) mapping of surficial sediment texture and clay mineralogy (Figure 4-2 and 4-3). These maps show that: (1) the surficial sediments of the upper harbour and bays indenting the northern shore of the lower harbour are composed of muds; and (2) these muds have characteristics similar to upper harbour sediments. The fact that Parua Bay sediments also contain the montmorillonite-rich clays characteristic of the Portland cement works supports these findings (Millar 1980). Discharge records for the cement works also indicate that sediment inputs to the harbour from the plant during the 1960s and 1970s exceed sediment delivery to the harbour from rivers.

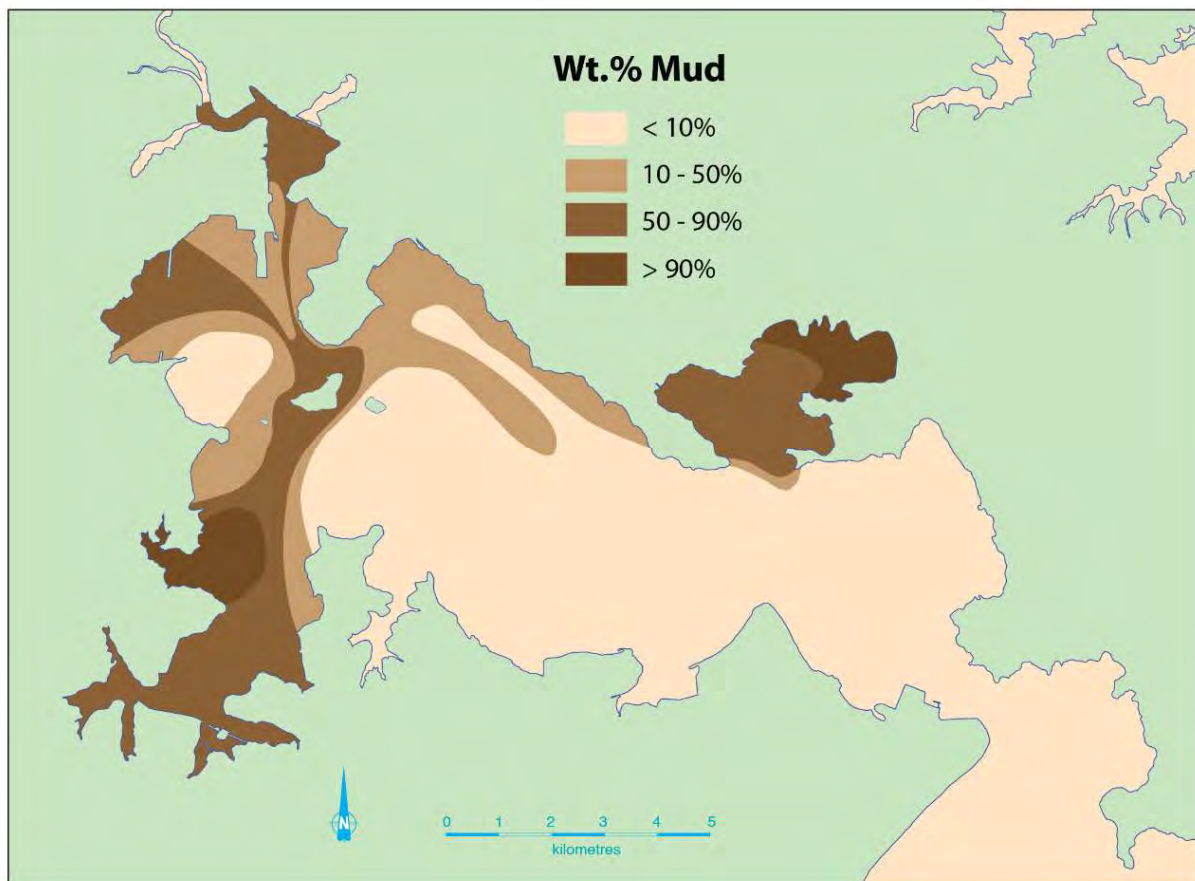


**Figure 4-2: Isopleth map of the percentage mud (by weight) in the surficial sediments of Whangarei Harbour (1978).** Reproduced from Millar (1980) with permission, Earth and Ocean Sciences Department, University of Waikato.

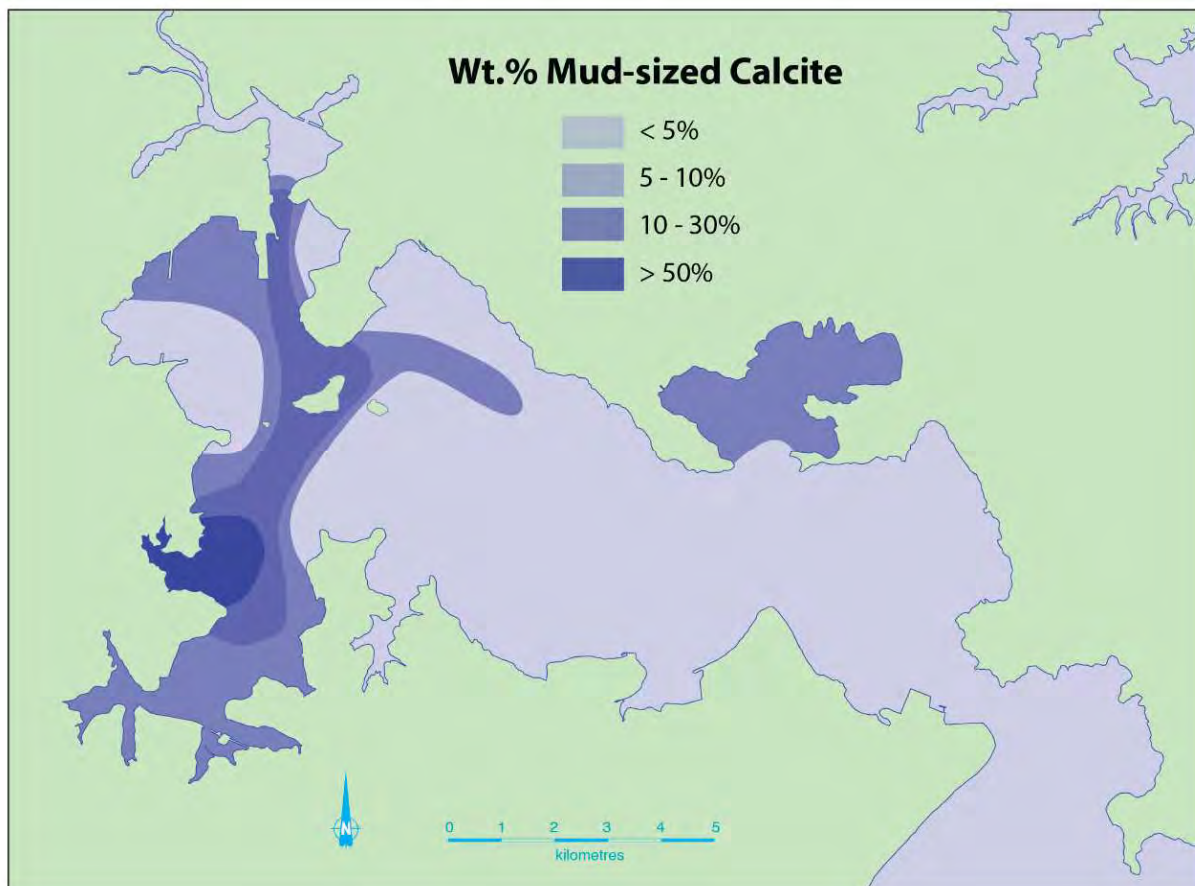


**Figure 4-3: Isopleth map of the percentage mud-sized calcite (by weight) in the surficial sediments of Whangarei Harbour (1978).** Reproduced from Millar (1980) with permission, Earth and Ocean Sciences Department, University of Waikato.

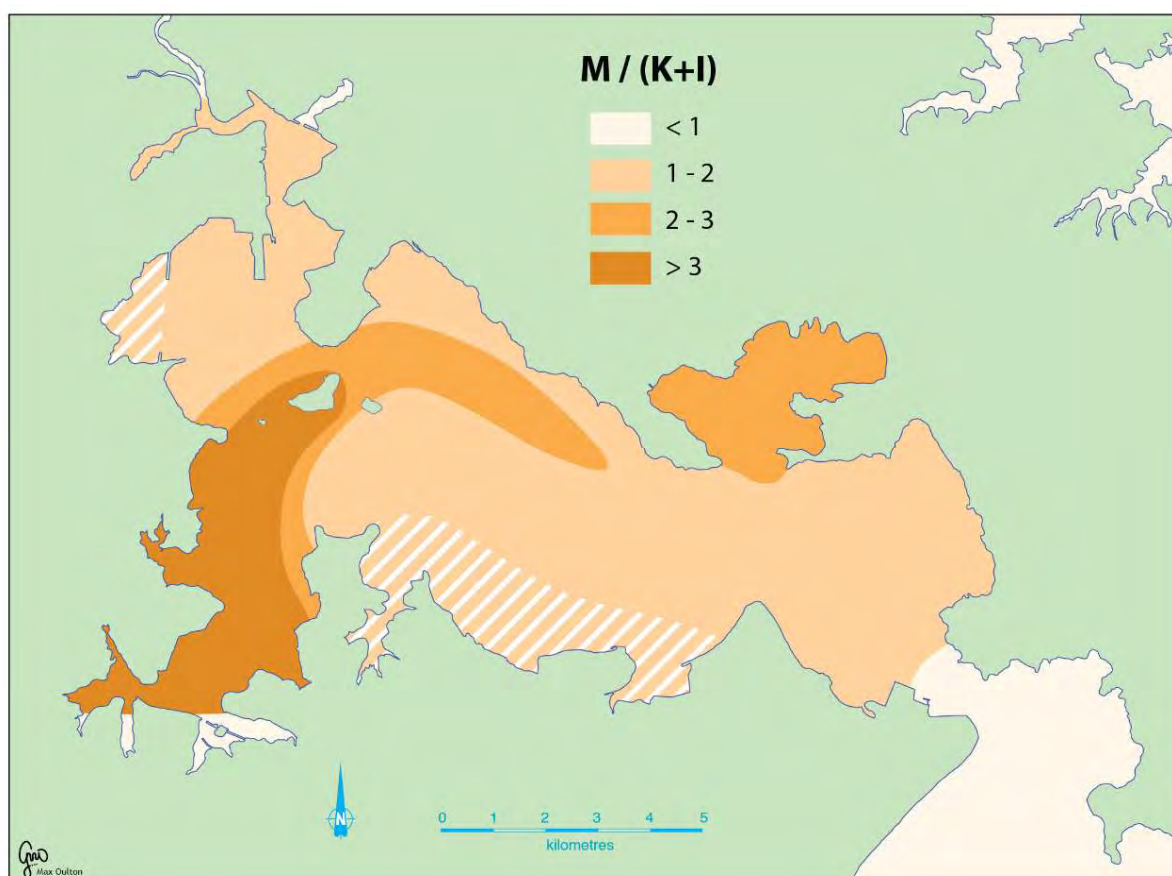


**Figure 4-4: Isopleth map of the ratio of montmorillonite (M) to kaolinite (K) and illite (I) clay-minerals in the surficial sediments of Whangarei Harbour (1978).** Reproduced from Millar (1980) with permission, Earth and Ocean Sciences Department, University of Waikato.

To the east of Parua Bay, the recent sedimentation history of Munro Bay also suggests that muds exported from the upper harbour is now impacting habitats remote from its source. The sediment core at Munro Bay (WHG-7) shows that mud began to deposit at this site from the mid-1950s, burying the previous shell-rich sands.

The modelling of the fatty-acid signatures from the various feasible sediment sources undertaken in the present study (Section 3.4) also show that present-day sedimentation in the upper harbour and along the northern shore of the lower harbour is dominated by sediments derived from the Hātea sub-catchment. Coastal sediments transported into the harbour by tidal currents dominate sedimentation in the lower harbour.

## 4.2 Sediment accommodation space and sea-level rise

The vertical accretion of intertidal flats through progressive sedimentation ultimately results in a reduction in sediment accumulation rates because:

- duration and frequency of tidal submergence (i.e., hydroperiod) and thus the potential for sediment delivery declines
- it follows that the accommodation space for sediment deposition (vertical offset between the tidal-flat surface elevation and the upper limit of the tide) progressive shrinks

- short-period waves characteristic of fetch-limited estuaries become increasingly effective at resuspending intertidal muds as water depth declines.

The effects of the negative feedback between intertidal-flat surface elevation and sediment accumulation rate is most pronounced on upper intertidal flats close to the upper-tidal limit. In these sedimentary environments, SAR approach the recent historical rate of relative sea-level rise in the absence of regional subsidence. Given its relatively stable tectonic setting, the rate of RSLR in Whangarei Harbour is likely to be similar to the long-term trend observed at the Port of Auckland ( $1.5 \pm 0.1$  mm/yr, Hannah & Bell 2012).

Future acceleration of sea-level rise predicted by various climate-change scenarios has the potential to increase sedimentation rates, particularly on the upper intertidal flats where sedimentation is most limited by hydroperiod.

The Ministry for the Environment (2008) provides sea-level-rise projections tailored for application in New Zealand for planning timeframes out to the 2090s (MfE, 2008). The accelerated SLR scenarios outlined in the MfE (2008) guidance document incorporate IPCC (2007) projections:

- Average SLR of 4.6 mm/yr resulting in an increase in sea level of 0.22 m by the 2050s and 5.4 mm/yr (+0.47 m) by the 2090s. This scenario represents a mid-range SLR projection.
- Average SLR of 6.9 mm/yr resulting in an increase in sea level of 0.33 m by the 2050s and 8.8 mm/yr (+0.77 m) by the 2090s. This scenario represents a possible upper-range SLR projection.

Research published after the IPCC (2007) assessment, including Hansen (2007), Rahmstorf et al. (2007) and Rignot et al. (2008) suggests that eustatic (global) sea-level increases of one metre or more could be possible by 2100 AD if ice-sheet melt rates accelerate. It is likely to be some time before the upper limit of potential sea level rise this century can be defined with some degree of confidence. The MfE (2008) manual recognises that local government must continue to make planning decisions in the coastal environment despite the uncertainty about future sea-level changes.

In Whangarei Harbour, sediment accumulation rates on the upper intertidal flats could potentially increase proportionally with these future projections of accelerated sea-level rise. The capacity of intertidal-flat habitats to keep pace with future SLR also depends on the rate of sediment supply. The primary sources of sediment to intertidal flats are: (1) future inputs of eroded catchment soils; (2) marine sands transported into the harbour by tidal currents; (3) estuarine sediments reworked by waves (e.g., lower intertidal and shallow subtidal); and (4) erosion of dune deposits fringing the southern shoreline of the lower harbour. In the upper harbour, sources (1) and (3) are likely to dominate whereas all of these potential sources are likely to supply sediments to intertidal-flats in the lower harbour.

The projected future rates of sea-level rise therefore represent the upper limit for sediment accumulation rates on the intertidal flats. There is substantial uncertainty in any estimates of future sediment supply rates as these are strongly couple with future climate (e.g., rainfall, wind, storm intensity and frequency) and land-use activities.

### 4.3 Influence of catchment deforestation on sedimentation rates

The effects of catchment deforestation on estuary sedimentation following the arrival of people in New Zealand ~700 years ago (e.g., Wilmshurst et al. 2008) has been reconstructed for a number of North Island estuaries using dated sediment cores. These previous studies indicate an order-of-magnitude increases in SAR following large-scale catchment deforestation, particularly over the last ~150 years (Goff 1997; Hume & McGlone, 1986; Hume & Dahm, 1992; Oldman & Swales, 1999; Swales & Hume, 1995; Swales et al. 1997, 2002a, 2002b, 2007a, 2011, 2012). These long-term sedimentation records have commonly been reconstructed using pollen and/or radiocarbon ( $^{14}\text{C}$ ) dating. Although this information is not available for Whangarei Harbour, recent data from a comprehensive study of the Bay of Islands system is instructive (Swales et al. 2012).

Radioisotope dating (i.e.,  $^{14}\text{C}$ ,  $^{210}\text{Pb}$ ,  $^{137}\text{Cs}$ ) of sediment cores from the Bay of Islands system show that SAR increased by an order of magnitude following large-scale catchment deforestation. Prior to deforestation, SAR averaged  $0.23 \pm 0.1 \text{ mm yr}^{-1}$  over the last ~10,000 years in comparison to  $2.5 \pm 0.8 \text{ mm yr}^{-1}$  (95% CI) during the last century. Long-term SAR also displayed similar spatial pattern to more recent sedimentation ( $^{210}\text{Pb}$  dating) with most rapid sedimentation occurring in the inlets close to the major river sources. The early infilling of the Mangapai and Hātea arms near the major river inputs to of Whangarei Harbour is consistent with this general pattern. Far-field transport and long-term accumulation of muds with low settling velocities (from the upper harbour) in the bays fringing the lower harbour is also a feature of sedimentation in the Bol system. Rapid deposition has occurred in Te Rawhiti Inlet (south-east Bol) over the last ~100 years, with a substantial proportion of this sediment most likely derived from the large but remote Kawakawa river (Swales et al. 2012).

### 4.4 Catchment sediment yield

The estimated specific sediment yield from the ~220 km<sup>2</sup> upper-harbour catchment of  $138 \pm 28 \text{ t/km}^2/\text{yr}$  ( $30,400 \pm 6040 \text{ t/yr}$ ) over the last 50 years (1962–2012) is within the range of values estimated by NIWA's WRENZ model for the major sub-catchments:  $122 \text{ t/km}^2/\text{yr}$  (Hātea),  $355 \text{ t/km}^2/\text{yr}$  (Otaika) and  $60 \text{ t/km}^2/\text{yr}$  (Mangapai). This estimate, largely based on sediment-core data, is similar to the WRENZ estimate for the Hātea sub-catchment, which accounts for 53% of the upper-harbour catchment. The total sediment mass retained in the upper harbour over the last 50 years (1962–2012), as estimated from the dated cores, is 1.5 million tonnes.

The historical clay-washing discharge from the Portland cement works (1918–1982) also needs to be considered in our assessment of catchment sediment yields over the last 50 years. Between 1958 and 1982 alone, when discharges from Portland ceased, an estimated 2.1 million tonnes (dry weight) of clay was discharged to the harbour. A large proportion of this clay, 60%, was delivered during the six years from 1966 to 1972 (section 1.4.2). This time period largely coincides with our assessment period for the upper-harbour catchment sediment yield. To place the Portland sediment input into context of the WRENZ catchment sediment yields estimates, average discharge rate from Portland between 1958 and 1982 was  $87,000 \text{ t/yr}$ . This rate is more than double the total  $38,000 \text{ t/yr}$  WRENZ estimate for the Hātea, Otaika and Mangapai sub-catchments.

Evidence presented in the present study as well as the previous work of Millar (1980) suggest that a large fraction of the Portland clay washing were exported from the upper to

the lower harbour. Some of this slurry would have almost immediately been flushed from the upper-harbour by ebb-tide currents. A proportion of the Portland-clay deposited on upper-harbour intertidal flats would also have been winnowed by waves and exported to the lower harbour. Portland clay deposited in mangroves and saltmarsh habitats are likely to have been permanently trapped. Stable-isotope data show that the present-day distribution of Portland sediments is limited to the intertidal flats in the immediate vicinity of the Portland wharf and mirrors the historical deposition pattern (sections 3.4, 4.4). Montmorillonite-rich clay (characteristic of the Portland sediments) was also detected in surficial sediments throughout the lower harbour, and Parua Bay in particular, towards the end of the time period when discharges from Portland occurred (section 4.1). Sediment-transport modelling conducted in the present study also indicates that fine suspended sediments are exported from the upper harbour and preferentially deposited in the bays and inlets flanking the lower harbours northern shoreline (section 3.1).

This assessment suggests that the specific sediment yield of  $138 \pm 28$  t/km<sup>2</sup>/yr ( $30,400 \pm 6040$  t/yr, 1962–2012) estimated for the upper-harbour catchment from the dated cores includes a historical contribution from the Portland Cement Plant. Information on the clay mineralogy and/or stable-isotope (FAME) signatures of these dated cores would enable the relative contributions of Portland versus catchment fine-sediments to be determined.

## 4.5 Comparison of sedimentation rates in North Island estuaries

Comparison of historical sediment accumulation rates measured in Whangarei Harbour with rates observed in other North Island estuaries enables data from the present study to be placed in a wider context of human impacts on New Zealand estuaries over the last ~100 years.

To ensure valid comparisons are made, only <sup>210</sup>Pb SAR data based on similar sampling and analysis methods are included. Environments include intertidal and subtidal flats in estuaries and coastal embayments (Swales 2002b, 2005, 2007a, 2008a, 2010, 2011, 2012). It should also be recognised that these data represent environments where long-term fine-sediment accumulation occurs. There are also environments where this does not occur. In large estuaries with fetches of several km or more waves, and to a lesser extent tidal currents, control fine-sediment transport and fate on intertidal and shallow subtidal flats (e.g., Green et al. 2007). In Whangarei Harbour, SAR are generally lower on intertidal flats with large wave fetches (e.g., west of Limestone Island) and remote from the major sediment sources in the upper harbour (e.g., Takahiwai).

### 4.5.1 Comparison of <sup>137</sup>Cs and <sup>210</sup>Pb SAR

Figure 4-5 compares SAR estimated from <sup>137</sup>Cs and <sup>210</sup>Pb dating for North Island estuaries, including Whangarei Harbour. It is evident that there is substantial scatter in the data. There is a general pattern of <sup>210</sup>Pb SAR being higher than <sup>137</sup>Cs SAR particularly for <sup>210</sup>Pb SAR >6 mm/yr at most core sites in the sampled estuaries.

The <sup>210</sup>Pb estimates of sediment accumulation rates are generally considered to be more reliable. This is because sediment dating is based on regression fits to the excess <sup>210</sup>Pb data and therefore has a statistical basis rather than purely relying on the reliability of a marker horizon as is the case for <sup>137</sup>Cs (Section 3.2.2). In some situations the <sup>210</sup>Pb SAR estimate may overestimate the “true” value if recent (i.e., high activity) <sup>210</sup>Pb is mixed deeply into the

seabed. This results in a steeper profile and therefore a higher apparent SAR value. In most cases, however, the SML is a small fraction of the excess  $^{210}\text{Pb}$  profile depth so that  $^{210}\text{Pb}$  SAR provide the most reliable estimates.

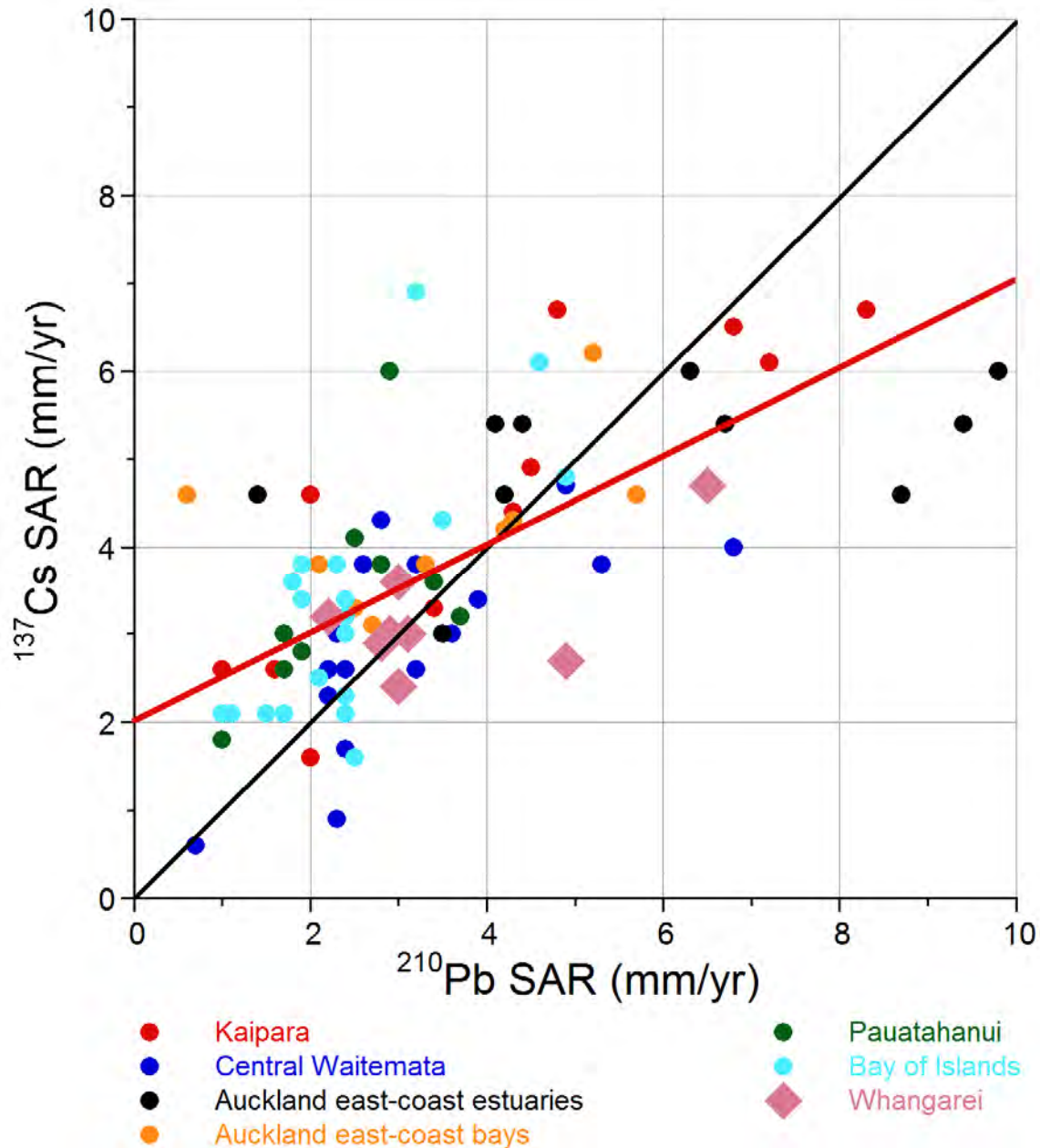


**Figure 4-5: Comparison of  $^{210}\text{Pb}$  and  $^{137}\text{Cs}$  sediment accumulation rates (SAR) in North Island estuaries.** Linear regression fit (red line) to entire data set:  $y = 0.48x + 2.05$  ( $P < 0.001$ ,  $r^2 = 0.46$ ,  $n = 87$ ) relative to 1:1 fit (black line).

Several factors suggest that the  $^{137}\text{Cs}$  data should be used with caution: (1)  $^{137}\text{Cs}$  activity has substantially reduced even since the  $^{137}\text{Cs}$  deposition peak in the early-1960s (i.e.,  $t_{1/2} = 30$  years) so that  $^{137}\text{Cs}$  activities are below detectable levels in deeper deposits and the  $^{137}\text{Cs}$  SAR is under-estimated; (2) deep sediment mixing (i.e., 5–20 cm) is indicated by  $^{137}\text{Pb}$  profiles at some sites, with the result that the maximum  $^{137}\text{Cs}$  overestimates SAR; (3) the early-1960s  $^{137}\text{Cs}$  deposition peak observed in New Zealand wetland deposits (Gehrels et al.

2008), and the most reliable  $^{137}\text{Cs}$  marker for dating, is absent in NZ estuarine and coastal marine sediments (Appendix C).

#### 4.5.2 Comparison of average $^{210}\text{Pb}$ SAR in North Island estuaries

Figure 4-6 presents data on the average  $^{210}\text{Pb}$  SAR for North Island estuaries based on data from 94 core sites. The Auckland east-coast data set includes the Mahurangi, Puhoi, Okura and Te Matuku estuaries and the Karepiro, Whitford and Wairoa embayments. The Bay of Islands as well as data from Whangarei Harbour in water depths of 1–100 m. Table 4-1 provides additional information.

The average  $^{210}\text{Pb}$  SAR in the Whangarei Harbour system is 3.4 mm/yr (SE = 0.48 mm/yr), which is in the mid-range for other North Island estuaries in the data set. The lowest average SAR occur in the central Bay of Islands where  $^{210}\text{Pb}$  SAR have averaged 1.9 mm/yr (SE = 0.2 mm/yr) over the last century.

Average SAR in the Kaipara Harbour (6.7 mm/yr) is substantially higher than in the other systems, although this result is skewed by high SAR values at two sites (20–30 mm/yr) and also results in large variability in the average SAR estimate. These high SAR sites appear to reflect local environmental conditions (e.g., lateral shift in channel position, proximity to river mouth) rather than due to increased catchment sediment load.

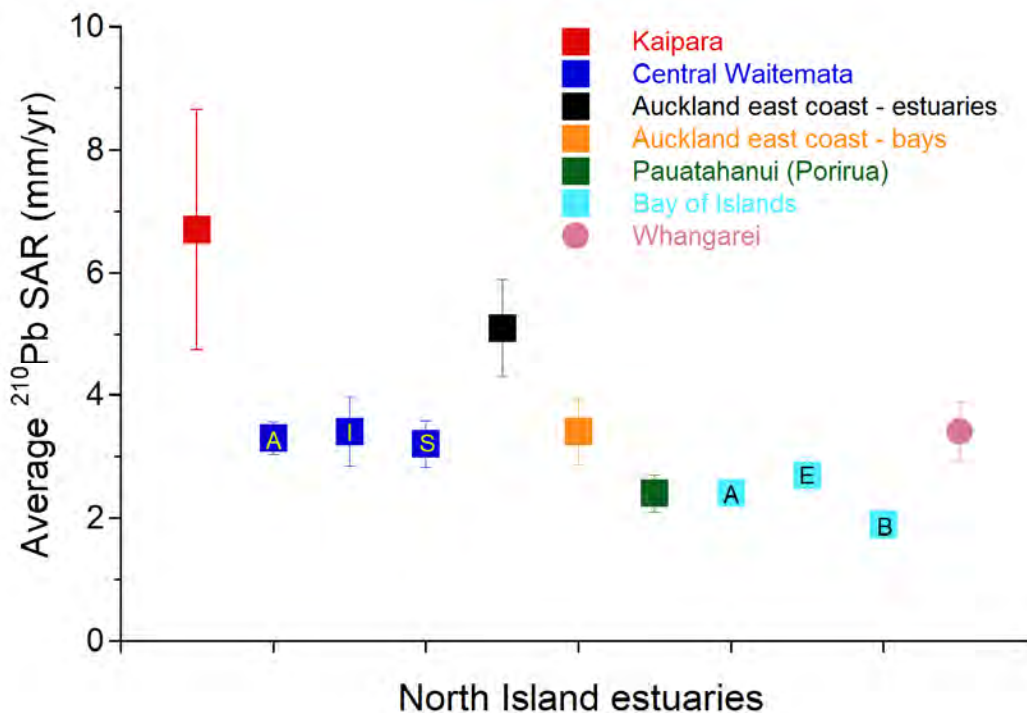


**Figure 4-6: Comparison of average  $^{210}\text{Pb}$  sediment accumulation rates (SAR) in North Island estuaries with standard errors shown.** Notes: (1) key - all data (A), intertidal sites (I), subtidal sites (S), estuaries (E), coastal embayments (B); (2) Total number of cores = 94; (3) Data sources: Table 4-1.

The average SAR in Whangarei Harbour is intermediate between intertidal habitats (5.1 mm/yr, SE = 0.8) and subtidal habitats (3.4 mm/yr, SE = 0.5) in Auckland east-coast estuaries. Figure 4-6 also shows that average  $^{210}\text{Pb}$  SAR are significantly lower in all other North Island estuaries and embayments (range 1.9–3.4 mm/yr) for which we have reliable data.

The data set also shows that small estuaries with limited sediment accommodation space relative to sediment-supply rate are most vulnerable to sediment infilling. Many of the Auckland east-coast estuaries fall into this category and have rapidly infilled with sediments from developing catchments. In larger estuaries with sufficient fetch for wave generation, the rate of estuary infilling is moderated by fine-sediment winnowing by waves. The Central Waitemata harbour is one example, where intertidal muds are redistributed by waves and tidal currents and deposited in subtidal habitats (Oldman et al. 2007). Further evidence of the key role that waves play in moderating estuary infilling comes from the Pauatahanui Inlet (Porirua), a small (4.6 km<sup>2</sup>), shallow subtidal estuary (Swales et al. 2005). Despite the fact that the Inlet receives runoff from a relatively large (109 km<sup>2</sup>) steep-land catchment, silt plumes during floods are observed to discharge from the inlet. Fine sediment deposited in the Inlet is also frequently resuspended by waves, even in the central basin, so that a substantial proportion of the terrigenous sediment load is exported from the Pauatahanui Inlet to the open sea.

**Table 4-1: Summary of average  $^{210}\text{Pb}$  sediment accumulation rates (SAR) and standard error (SE) in North Island estuaries and coastal embayments over the last 50–100 years.** The total number of cores = 94. Key: Central Waitemata Harbour (CWH), Bay of Islands (Bol), East Coast (EC)

Estuary	n	Habitat	$^{210}\text{Pb}$ SAR (mm yr <sup>-1</sup> )	$^{210}\text{Pb}$ SAR-SE (mm yr <sup>-1</sup> )	Source
Whangarei	9	Intertidal & subtidal	3.4	0.5	Present study
Kaipara	16	intertidal	6.7	1.9	Swales et al. (2011)
CWH - all data	18	intertidal & subtidal	3.3	0.3	Swales (2002b, 2007)
CWH - intertidal	10	intertidal	3.4	0.6	–
CWH - subtidal	8	subtidal	3.2	0.4	–
Auckland EC estuaries	13	intertidal	5.1	0.8	Swales (2002b, 2007a)
Auckland EC bays	9	subtidal	3.4	0.5	Swales (2002b, 2007a, 2008a)
Pauatahanui	9	subtidal	2.4	0.3	Swales (2005)
Bol – all data	20	subtidal	2.4	0.2	Present study
Bol – inlets	14	subtidal	2.7	0.3	
Bol – embayment	6	subtidal	1.9	0.2	

The mid-range average SAR measured in Whangarei Harbour is consistent with the sedimentation history of this system.  $^{210}\text{Pb}$  dating of sediment cores indicates that sediment accumulation rates reduced in the upper harbour and Parua Bay in the early–mid 1900s. This is most likely due to the reduction in sediment delivery and sediment accommodation space associated with the progressive vertical accretion of intertidal flats close to major sub-catchment outlets. There is some evidence that sediments from the upper-harbour catchments began to accumulate in the lower harbour, particularly in bays and inlets fringing

the northern shore of the harbour. For example, muds began to accumulate in Munro Bay from the early 1950s (WHG-7) and CSSI analysis indicates that a substantial proportion of these muds are derived from the Hātea sub-catchment. Mud-transport modelling as well as the earlier work of Millar (1980) also indicate preferential deposition of muds along the northern harbour shore.

## 4.6 Sediment sources

While sediment accumulation rates in Whangarei Harbour provide an estimate of how much sediment is being deposited at different locations in the harbour they do not identify where the sediment is coming from. The CSSI technique provides that source identification within the limitations of the method. The Whangarei Harbour receives terrigenous sediment from three main river inflows, the Hātea River, the Otaika River and the Mangapai Stream. Because the CSSI technique uses the top-most 2 cm of the sediment which is totally within the surface mixed layer, the results are an integration of all sediment inputs from all land-use practises that have occurred over the last 3 to 6+ years and do not only reflect the sediment from the last catchment erosion/harbour sedimentation event.

### 4.6.1 Sediment dispersion across the harbour

The patterns of sediment dispersion across the harbour identified by the CSSI technique indicate that, although the Otaika River system has a larger catchment than the Hātea River, in recent years the Hātea River inflow has had a wider spatial influence on the inner harbour sediment. The Mangapai Stream inflow appears to be a minor sediment sources, which indicates that the Mangapai arm of the harbour is likely to be a deposition zone for fine sediment from the other two inflows.

The spatial pattern of sediment dispersion from the Otaika River (Figure 3-17) was consistent with the output from the mud transport model (Figure 3-20) and the area of sediment influenced by the Portland isotopic signature (Figure 3-20) was consistent with the zone of influence determined geochemically (Figure 4-7).

Because the historical sediment discharges from the Portland cement works have ceased, the presence of this locally strong isotopic signature implies that it is a legacy effect. The most likely source of the Portland labelled sediment is in situ mixing by physical and biological processes. In particular, remobilisation of surficial sediments by locally generated waves and bioturbation by infauna within the surface-mixed layer is indicated by <sup>7</sup>Be data and x-ray images of cores as well as field observations (sections 3.2.1, 3.3). Bioturbation by mud crabs, which excavate sediment from burrows as deep as 30 cm, and polychaetes (worms), which also bring deep sediments to the surface. Other bioturbators include sting rays which feed on the polychaetes and crabs by blowing “pits” as deep as 20 cm into the sediment to dislodge these and other biota.

Crab burrows, polychaete tubes and ray pits were observed in large numbers throughout most of the upper harbour intertidal zone, with new crab burrows overlapping older burrows (Figure 4-8). This level of bioturbation implies that older sediment deposits are likely to be reworked and mixed with contemporary sediments is likely to occur over large areas of intertidal flat in the upper harbour.

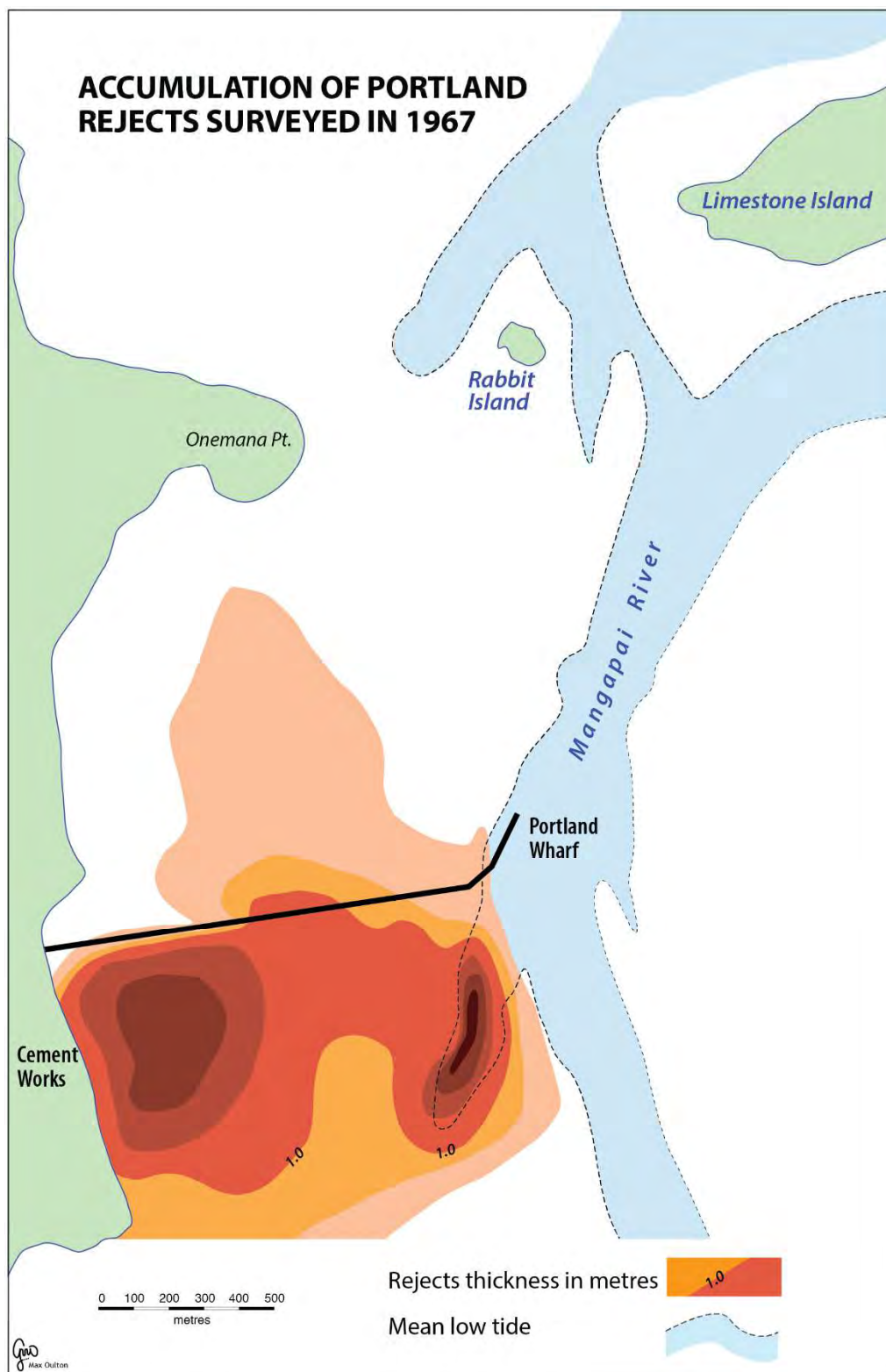


**Figure 4-7: Contour map of the thickness of Portland cement works deposits in the Mangapai arm as surveyed in 1967.** Reproduced from Millar (1980) with permission, Earth and Ocean Sciences Department, University of Waikato.

In the lower harbour there were local variations in sediment patterns around small stream inputs but, in general, the surficial sediment were dominated by coastal sources. This implies that long shore drift along the coast may be causing sediment accumulation in the outer harbour.

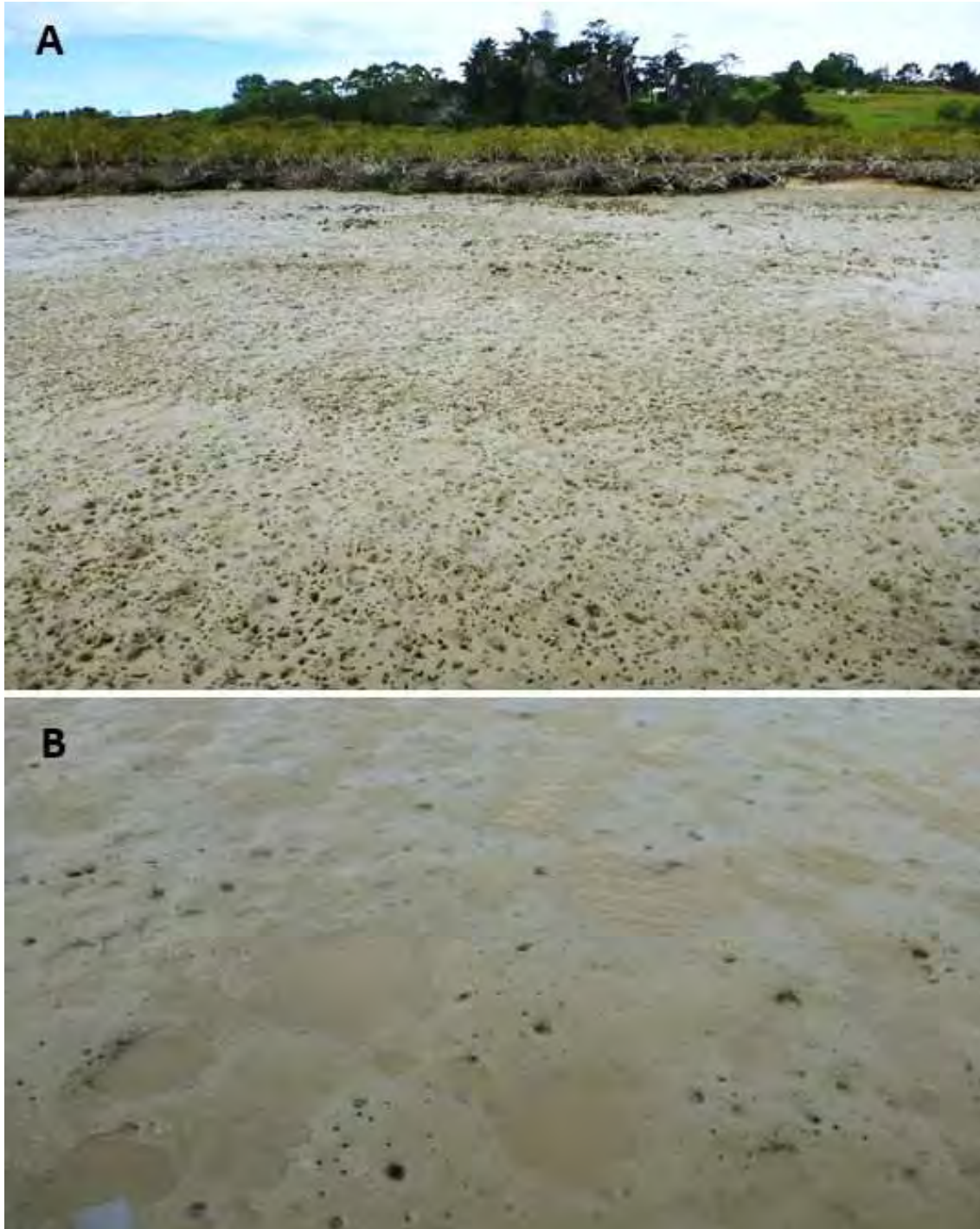


**Figure 4-8: Evidence of extensive bioturbation in the intertidal zone of the upper harbour.** A) Extensive crab burrows and polychaete tubes, B) crab burrows and ray pits in the soft mud.

#### 4.6.2 Catchment sources

Contemporary sources of terrigenous sediments depositing in Whangarei Harbour were determined from analysis and modelling of the stable isotope signatures of Fatty Acid soil biomarkers. The results of this work indicate that sediments derived from the Hātea sub-catchment are the most widely dispersed and are presently accumulating in the upper and middle-reaches of Whangarei Harbour. The spatial distribution pattern indicates that sediment from the Hātea River system is also dispersed east along the northern shores beyond the Onerahi Peninsula. Sediments derived from Otaika and the Mangapai sub-catchments and Portland cement works are locally accumulating near these sources. It is notable that Portland sediments were present in the surficial sediments of Parua Bay and elsewhere in the middle reaches of the harbour in the late 1970s (Millar 1980). This indicates that these montmorillonite-clay rich sediments were more widely dispersed during the 74 years (1918–1982) that the cement plant discharged reject washings to the upper harbour. The present-day distribution of the Portland sediments reflects the large quantities of material deposited in the Mangapai arm close to the source.

Evaluation of surficial sediments deposited at the outlets of the major river sources enables the likely present-day contribution of various land uses to harbour sedimentation to be quantified. The soil contributions from the various sources evaluated from the CSSI data are reported here to the nearest whole percent.

It should be noted that the analysis of the stable-isotope data show a substantial change in the sources of sediment deposited in the tidal reach of the Hātea River south of Mair Park. There are several potential reasons for this “isotopic disconnect” between the upper Hātea catchment soils and the harbour sediments: (1) The sediment-source modelling may not have included all potential sources, e.g., the harbour sediments Hātea-arm are likely to include “urban sediments” eroded during the development of the city; (2) historical sediment deposits are also likely to have been reworked and mixed with more recent sediments by dredging and reclamation works associated with the extensive port development that occurred from the 1950s onwards. These older sediment deposits are isotopically enriched relative to contemporary sediments most likely due to the Suess effect (section 2.5.4). Therefore, this reworking of sediment deposits will result in a blended stable-isotope signature, a mixture of old and new. The data presented in this report suggests that upper-harbour sediments were exported to the lower harbour from the 1950s onwards. These exported sediments would have included reworked sediments with a blended stable-isotope signature from the tidal reach of the Hātea River. The results of the analysis of the Hātea River sediment sources are interpreted in line with these considerations.

The major sources of sediment by land use and sub-catchment have been evaluated for the Hātea, Otaika and Mangapai catchments. Sub soils derived from stream-bank erosion, gullyng and slips are major sources of sediments deposited in stream beds and at river deltas in the upper harbour. Native forest and pasture are the other primary sources of sediment. The contributions from pasture and subsoil are likely to reflect bank erosion by stock direct access to streams (Figure 4-9) rather than erosion from flat paddocks.



**Figure 4-9: Bank erosion (A) slumping caused by stock tracks down to the stream; (B) trampling of the stream edge by cattle and dairy cows.**

### Hātea River

- Almost all (>90%) of the recent sediment in the Hātea River at Mair Park came from the catchment upstream of Tikipunga with <10% coming from the Otangarei Stream system and the steep forest land on the eastern side of the river. That sediment is composed of soils from pine forest (24%), pasture of all types (11%), pasture sub-soil (7%) and native forest including totara (59%). It should be noted that the soils under pasture that has recently been established following deforestation will retain the stable-isotope signature of the original forest for several years or more.
- Assessment of the sediment sources to the Hātea River Delta site showed that a maximum of 9% of these delta sediments came from the upper Hātea River. The Awaroa and Waioneone Creeks contributed up to 3%, Limeburners Creek contributed up to 31% and the Raumanga Stream system contributed up to 56%.
- The disproportionately low proportion of upper Hātea River sediment in the river delta sample is most likely due to the blending of stable-isotope signatures associated with the disturbance of delta sediment deposits resulting from the extensive dredging and reclamation works at the Port of Whangarei since the 1950s. The few mm of recent Hātea sediment would be diluted by this blended sediment in the 20-mm thick surficial sediment samples that were analysed.
- In the Raumanga Stream, most (90%) of the stream sediment were composed of sub-soils most likely derived from bank erosion and slips in the Maunu Road tributary. This source potentially includes the Waiarohia Stream although the latter was not sampled. The main Raumanga Stream contributed up to 5% as subsoil with up to 4% native forest including totara. Pasture signature was present but at <1 %.

- In Limeburners Creek up to 90% of stream sediments was composed of subsoil of the type found along the Maunu Road tributary (45%) and the main Raumanga Stream (44%) with up to 10% as native forest including Totara.

### **Otaika River**

- The Otaika River delta receives sediment from the main Otaika River system (80%) and the Puwera Stream system (20%). Modelling of the CSSI data shows that 65% of the sediment comes from the upper catchment (above the Puwera Stream confluence), including the Otakaranga Stream catchment and the Otaika Valley streams. The remaining sediment is contributed from pasture (25%) and native forest (8%) on the steeper northern hills.
- The Otaika Valley river catchment above the confluence with the Otakaranga Stream produces 12% of the upper catchment sediment, mostly from pasture with an underlying native forest (totara) signature. The Otakaranga Stream catchment contributes 86% of the sediment. The Otakaranga Stream sediment is composed of sediments eroded from pasture (11%), bank erosion (19%) and native-forest soils (69%). The large native-forest soil contribution most likely reflects the relatively recent clearing of native forest and conversion to pasture.
- Deconstruction of the Puwera Stream sediment sources showed that 94% were subsoils which may have been derived from bank erosion or recent slips. There was a small proportion of pine (4%) and traces of pasture and native forest soils present.

### **Mangapai River**

- Sediment in the Mangapai River delta was collected at core site WHG-1. The catchment sediment source contributions were evaluated using the land-use soil (stable-isotope) signatures. The results indicate that around 75% of the sediment was derived from bank erosion, which includes dirt roads and road cuttings. The rest of the sediment came from pine forestry (10%), pasture (7%) and native forest (8%).

## 5 Acknowledgements

The authors thank the following NRC staff who assisted with collection of sediment samples: Richard Griffiths, Wayne Teal, Ricky Eyre, and Marcus Schlesier. Ben Tait (NRC Planner) also contributed to project planning and scoping. NRC gratefully acknowledge MBIE Envirolink (Medium advice grant, contract C01X1210) and Northport for co-funding this study. Dr Terry Hume (NIWA) reviewed this report. Max Oulton (Cartographer, University of Waikato) prepared some of the maps and diagrams for this report. We thank the Department of Earth and Ocean Sciences, University of Waikato for granting permission for NIWA to reproduce sediment maps from: Millar, A.S. (1980). The Hydrology and Surficial Sediments of Whangarei Harbour, Master of Science thesis.

## 6 References

- Alexander, C.R., Smith, R.G., Calder, F.D., Schropp, S.J., Windom, H.L. (1993) The historical record of metal enrichment in two Florida estuaries. *Estuaries*, 16(3B): 627–637.
- Benoit, G., Rozan, T.F., Pattoon, P.C., Arnold, C.L. (1999) Trace metals and radionuclides reveal sediment sources and accumulation rates in Jordan Cove, Connecticut. *Estuaries*, 22(1): 65–80.
- Blake, W.H., Ficken, K.J., Taylor, P., Russell, M.A., Walling, D.E. (2012) Tracing crop-specific sediment sources in agricultural catchments. *Geomorphology*, 139–140: 322–329.
- Bromley, R.G. (1996) *Trace fossils: biology, taphonomy and applications*, second edition. Chapman and Hall, London: 361.
- Ferrar, H.T. (1925) The geology of the Whangarei–Bay of Islands Subdivision, Kaipara Division. Department of Mines. *Geological Survey Branch*, Bulletin No. 27 (New Series), W.A.G. Skinner, Government Printer, Wellington.
- Gehrels, W.R., Hayward, B.W., Newnham, R.M., Southall, K.E. (2008) A 20th century acceleration of sea-level rise in New Zealand. *Geophysical Research Letters*, 35, L02717, doi:10.1029/2007GL032632.
- Gibbs, M., Hewitt, J. (2004) Effects of sedimentation on macrofaunal communities: a synthesis of research studies for ARC. Prepared by NIWA for Auckland Regional Council, *NIWA Client Report* HAM2004-060.
- Gibbs, M., Olsen, G. (2010) Chapter 5: Determining sediment sources and dispersion in the Bay of Islands. Bay of Islands OS20/20 survey report. Prepared by NIWA for LINZ, *Client Report Number* WLG2010-38: 30.
- Gibbs, M. (2006a) Source mapping in Mahurangi Harbour. *Auckland Regional Council Technical Publication*, TP321.
- Gibbs, M. (2006b) Whangapoua Harbour sediment sources. *Environment Waikato Technical Report*, No. 2006/42: 49.
- Gibbs, M. (2008) Identifying source soils in contemporary estuarine sediments: a new compound specific isotope method. *Estuaries and Coasts*, 31: 344–359.
- Gibbs, M., Bremner, D. (2007) Wharekawa Estuary sediment sources. *NIWA Client Report* HAM2007-111 for Environment Waikato.
- Gibbs, M., Elliott, S., Basher, L. (2008) Sediment source identification and apportionment by land-use: testing a new stable isotope technique in the Waitetuna River catchment. *Poster paper presented at the IAHS-ICCE International Symposium*, 1–5 December, Christchurch, New Zealand.
- Gibbs, M., Funnell, G., Pickmere, S., Norkko, A., Hewitt, J. (2005) Benthic nutrient fluxes along an estuarine gradient: influence of the pinnid bivalve *Atrina zelandica* in summer. *Marine Ecology Progress Series*, 288: 151–164.

- Goff, J.R. (1997) A chronology of natural and anthropogenic influences on coastal sedimentation, New Zealand. *Marine Geology*, 138: 105–117.
- Goldberg, E.D., Kiode, M. (1962) Geochronological studies of deep sea sediments by the ionium/thorium method. *Geochemica et Cosmochimica Acta*, 26: 417–450.
- Green, M.O., Black, K.P., Amos, C.L. (1997) Control of estuarine sediment dynamics by interactions between currents and waves at several scales. *Marine Geology*, 144: 97–116.
- Guinasso, N.L. Jr., Schink, D.R. (1975) Quantitative estimates of biological mixing rates in abyssal sediments. *Journal of Geophysical Research*, 80: 3032–3043.
- Hannah, J., Bell, R.G. (2012) Regional sea-level trends in New Zealand. *Journal of Geophysical Research*, 117: C01004, doi:10.1029/2011JC007591.
- Hume, T.M., McGlone, M.S. (1986) Sedimentation patterns and catchment use changes recorded in the sediments of a shallow tidal creek, Lucas Creek, Upper Waitemata Harbour, New Zealand. *Journal of the Royal Society of New Zealand*, 19: 305–317.
- Hume, T.M., Dahm, J. (1992) An investigation of the effects of Polynesian and European land use on sedimentation in the Coromandel estuaries. Water Quality Centre, *DSIR consultancy report*, 6104, prepared for the Department of Conservation.
- IPCC (2007). Summary for Policymakers. In: *Climate Change 2007: Synthesis Report*. An Assessment of the Intergovernmental Panel on Climate Change approved at IPCC Plenary XXVII (Valencia, Spain, 12–17 November). [http://www.ipcc.ch/pdf/assessment-report/ar4/syr/ar4\\_syr.pdf](http://www.ipcc.ch/pdf/assessment-report/ar4/syr/ar4_syr.pdf)
- Lohrer, A.M., Hewitt, J.E., Thrush, S.F., Lundquist, C.J., Nicholls, P.E., Liefing, R. (2003) Impact of terrigenous material deposition on subtidal benthic communities. ARC Technical report 217. *NIWA Client Report* HAM2003-055.
- Matthews, K.M. (1989) Radioactive fallout in the South Pacific, a history. Part 1. Deposition in New Zealand. *Report NRL 1989/2*. National Radiation Laboratory, Christchurch, New Zealand.
- McGlone, M.S. (1983) Polynesian deforestation of New Zealand: a preliminary synthesis. *Archaeology in Oceania*, 18: 11–25.
- Middleton, A. (2003) Māori and European landscapes at Te Puna, Bay of Islands, New Zealand, 1805–1850. *Archaeology in Oceania*, 38: 110–124.
- Millar, A.S. (1980) *Hydrology and surficial sediments of Whangarei Harbour*. Master of Science thesis, Department of Earth Sciences, University of Waikato, New Zealand: 212.

- Ministry for the Environment (2008) Coastal hazards and climate change. A *guidance manual for local government in New Zealand*, 2<sup>nd</sup> Edition. Ministry for the Environment, Wellington.
- Morton J.E., Miller, M.C. (1973) *The New Zealand Sea Shore*, Second Edition. William Collins and Sons, Glasgow.
- Needham H.R., Pilditch C.A., Lohrer A.M. & Thrush S.F. (2012). Density and habitat dependent effects of crab burrows on sediment erodibility. *Journal of Sea Research*, 76: 94-104.
- New Zealand Soil Bureau (1968) Soils of New Zealand, Parts 1, 2, 3. *New Soil Bureau*, 26.
- Northland Regional Council (1989) *Whangarei harbour study*. Prepared by Whangarei Harbour Study Working and Steering Committees for the Northland Harbour Board: 292.
- Oldman, J.W., Swales, A. (1999) Maungamaungaroa Estuary numerical modelling and sedimentation. *NIWA Client Report* ARC70224, prepared for Auckland Regional Council.
- Phillips, D.L. Gregg, J.W. (2003). Source partitioning using stable isotopes: coping with too many sources. *Oecologia*, 136: 261–269.
- Powell A.W.B. (1979) *New Zealand Mollusca: marine, land and freshwater shells*. Collins, Auckland: 500.
- Rahmstorf S. (2007). A semi-empirical approach to projecting sea-level rise. *Science* 315: 368-370.
- Reeve, G., Pritchard, M., Ramsay, D. (2010) Whangarei Harbour hydrodynamic and dispersion model: Model set-up, calibration and validation. *NIWA Client Report* HAM2009-154, for Northland Regional Council, North Port and Whangarei District Council.
- Rignot, E.; Bamber, J.L.; Van der Broeke, M.R.; Davis, C.; Li, Y.; Van der Berg, W.J.; Van Meijgaard, E. (2008). Recent Antarctic ice mass loss from radar interferometry and regional climate modelling. *Nature Geoscience*, 1: 106–110.
- Ritchie, J.C., McHenry, J.R. (1989) *Application of radioactive fallout caesium-137 for measuring soil erosion and sediment accumulation rates and patterns: A review with bibliography*. Hydrology Laboratory, Agriculture Research Service, U.S. Department of Agriculture, Maryland.
- Robbins, J.A., Edgington, D.N. (1975) Determination of recent sedimentation rates in Lake Michigan using <sup>210</sup>Pb and <sup>137</sup>Cs. *Geochimica et Cosmochimica Acta*, 39: 285–304.
- Sharma, K., Gardner, L.R., Moore, W.S., Bollinger, M.S. (1987) Sedimentation and bioturbation in a saltmarsh revealed by <sup>210</sup>Pb, <sup>137</sup>Cs and <sup>7</sup>Be studies. *Limnology and Oceanography*, 32(2): 313–326.

- Sheffield, A.T., Healy, T.R., McGlone, M.S. (1995) Infilling rates of a steepland catchment estuary, Whangamata, New Zealand. *Journal of Coastal Research*, 11(4): 1294–1308.
- Sommerfield, C.K., Nittrouer, C.A., Alexander, C.R. (1999) <sup>7</sup>Be as a tracer of flood sedimentation on the Northern California margin. *Continental Shelf Research*, 19: 335–361.
- Swales, A., Hume, T.M. (1995) Sedimentation history and potential future impacts of production forestry on the Wharekawa estuary, Coromandel Peninsula. *NIWA Client Report CHH003* for Carter Holt Harvey Ltd.
- Swales, A., Hume, T.M., Oldman, J.W., Green, M.O. (1997) Holocene sedimentation and recent human impacts in a drowned-valley estuary: 895–900. In: Lumsden, J. (Ed.). *Proceedings of the 13<sup>th</sup> Australasian Coastal and Ocean Engineering Conference*, Centre for Advanced Engineering, University of Canterbury, Christchurch, New Zealand.
- Swales, A., Williamson, R.B., Van Dam, L.F., Stroud, M.J., McGlone, M.S. (2002a) Reconstruction of urban stormwater contamination of an estuary using catchment history and sediment profile dating. *Estuaries*, 25(1): 43–56.
- Swales, A., Hume, T.M., McGlone, M.S., Pilvio, R., Ovenden, R., Zviguina, N., Hatton, S., Nicholls, P., Budd, R., Hewitt, J., Pickmere, S., Costley, K. (2002b) Evidence for the physical effects of catchment sediment runoff preserved in estuarine sediments: Phase II (field study). *Auckland Regional Council Technical Publication*, 221. <http://www.arc.govt.nz/plans/technical-publications/technical-publications/technical-publications-201-250.cfm>.
- Swales, A., MacDonald, I.T., Green, M.O. (2004) Influence of wave and sediment dynamics on cordgrass (*Spartina anglica*) growth and sediment accumulation on an exposed intertidal flat. *Estuaries*, 27(2): 225–243.
- Swales, A., Bentley, S.J., McGlone, M.S., Ovenden, R., Hermansphan, N., Budd, R., Hill, A., Pickmere, S., Haskew, R., Okey, M.J. (2005) Pauatahanui Inlet: effects of historical catchment landcover changes on estuary sedimentation. *NIWA Client Report HAM2004-149*, for Wellington Regional Council and Porirua City Council.
- Swales, A., Stephens, S., Hewitt, J.E., Ovenden, R., Hailes, S., Lohrer, D., Hermansphan, N., Hart, C., Budd, R., Wadhwa, S., Okey, M.J. (2007a) Central Waitemata Harbour Study. Harbour Sediments. *Auckland Regional Council Technical Report*, 2008/034, [http://www.arc.govt.nz/plans/technical-publications/technical-reports/technical-reports-2008/technical-reports-2008\\_home.cfm](http://www.arc.govt.nz/plans/technical-publications/technical-reports/technical-reports-2008/technical-reports-2008_home.cfm).
- Swales, A., Bell, R.G., Ovenden, R., Hart, C., Horrocks, M., Hermansphan, N., Smith, R.K. (2007b) Mangrove-habitat expansion in the southern Firth of Thames: sedimentation processes and coastal-hazards mitigation. *Environment Waikato Technical Report*, 2008/13, [www.ew.govt.nz/Publications/Coastal/](http://www.ew.govt.nz/Publications/Coastal/).

- Swales, A., Gibbs, M., Ovenden, R., Budd, R., Hermanspahn, N. (2008a) Sedimentation in the Okura – Weiti – Karepiro Bay system. *Auckland Regional Council Technical Report*, 2008/026. [http://www.arc.govt.nz/plans/technical-publications/technical-reports/technical-reports-2008/technical-reports-2008\\_home.cfm](http://www.arc.govt.nz/plans/technical-publications/technical-reports/technical-reports-2008/technical-reports-2008_home.cfm).
- Swales, A., Bentley, S.J. (2008b) Recent tidal-flat evolution and mangrove-habitat expansion: application of radioisotope dating to environmental reconstruction. Sediment Dynamics in changing environments. (Proceedings of a symposium held in Christchurch, New Zealand, December 2008). *IAHS Publication*, 325: 76–84.
- Swales, A., Bell, R.G., Gorman, R., Oldman, J.W., Altenberger, A., Hart, C., Claydon, L., Wadhwa, S., Ovenden, R. (2009) Potential future changes in mangrove habitat in Auckland's east-coast estuaries. *NIWA Client Report HAM2008-030* for Auckland Regional Council.
- Swales, A., Gibbs, M., Ovenden, R., Costley, K., Hermanspahn, N., Budd, R., Rendle, D., Hart, C., Wadhwa, S. (2011) Patterns and rates of recent sedimentation and intertidal vegetation changes in the Kaipara Harbour. *NIWA Client Report HAM2011-040*.
- Swales, A., Gibbs, M., Hewitt, J., Hailes, S., Griffiths, R., Olsen, G., Ovenden, R., Wadhwa, S. (2012) Sediment sources and accumulation rates in the Bay of Islands and implications for macro-benthic fauna, mangrove and saltmarsh habitats. *NIWA Client Report HAM2012-048*.
- Valette-Silver, N.J. (1993) The use of sediment cores to reconstruct historical trends in contamination of estuarine and coastal sediments. *Estuaries*, 16(3B): 577–588.
- Wilson (N.Z.) Portland Cement Ltd (1978) *Submissions on behalf of application for rights to discharge wastewater in combination with works stormwater, and treated sewage wastewater*. Northland Regional Water Board, Whangarei.
- Wilmshurst, J.M., Anderson, A.J., Higham, T.F.G., Worthy, T.H. (2008) Dating the late prehistoric dispersal of Polynesians to New Zealand using the commensal rat. *Proceedings of the National Academy of Sciences*, 105(22): 7676–7680.
- Wise, S. (1977) The use of radionuclides  $^{210}\text{Pb}$  and  $^{137}\text{Cs}$  in estimating denudation rates and in soil measurement. *Occasional paper No. 7 University of London*, Kings College, Department of Geography, London.
- WRENZ (2007) NIWA Water Resources Explorer. <http://wrenz.niw.co.nz/webmodel/>
- Thrush, S.F., Hewitt, J.E., Cummings, V.J., Ellis, J.I., Hatton, C., Lohrer, A., Norkko, A. (2004) Muddy waters: elevating sediment input to coastal and estuarine habitats. *Frontiers in Ecology and Evolution*, 2: 299–306.

## Appendix A Location of sediment cores as recorded

Table A-1: Sediment cores collected in Whangarei Harbour, February and October 2012.

Site	Location description	Date	Time (NZST)	Water depth (m)	Latitude/ NZMG-N	Longitude/ NZMG-E	Core lengths (cm)
WHG-1	Mangapai arm	15/02/12	1222	1.7	35° 49.5951'S	174° 20.7303'E	163,155
WHG-2	Mangapai arm	15/02/12	1255	1.5	35° 48.7660'S	174° 20.6031'E	174,153
WHG-3	Mangapai arm	15/02/12	1117	0.6	35° 47.9463'S	174° 20.7440'E	57, 59
WHG-4	Hātea arm	14/02/12	1238	1.3	35° 47.0804'S	174° 20.713'E	66,185, 65
WHG-5	Hātea arm	14/02/12	1157	1.2	35° 46.5642'S	174° 20.3811'E	30,32
WHG-6	Hātea arm	14/02/12	1126	1.5	35° 45.8258'S	174° 20.4461'E	168,137
WHG-7	Munro Bay	16/02/12	1335	3.5	35° 47.3400'S	174° 29.2139'E	46,55
WHG-8	Takahiwai	02/12	low tide	0.0	6034564	1730526	54
WHG-10	Parua Bay	14/02/12	1002	3.4	35° 46.6890'S	174° 27.4848'E	110,105
WHG-11	Parua Bay	16/02/12	1227	–	35° 46.9716'S	174° 26.3820'E	110,160
WHG-12	Marsden Bay	16/02/12	–	LT	6033425N	1733453E	60,60
WHG-13	Parua Bay	14/02/12	1452	–	35° 47.0804'S	174° 26.7759'E	63,85,85
WHG-14	Hātea arm	05/10/12	–	LT	6041641	1722598	100,100

## Appendix B Details of samples collected for compound-specific stable isotope analysis

### Catchment sample locations

Easting (NZMG)	Northing (NZMG)	Site Code	Sample ID	Sample Description	Carbon (%)	delta C <sup>13</sup> /C <sup>12</sup>	c14:0	c16:0	c18:0	c18:1 w9c
1717992	6039069	OAKS-1	OA157-72	Otaika (below confluence with Puwera)	1.90	-26.02	-39.86	-31.12	-33.26	-32.64
1715790	6039780	OTAIKA-2	OA157-51	Otaika (above confluence with Puwera)	1.03	-27.18		-34.25	-31.44	
1714678	6040513	OTAIKA-3	OA157-52	Otaika (below Otakaranga Confluence)	0.49	-27.06				
1714620	6040309	OTAIKA-4	OA157-53	Otaika (Northern Tributary)	0.86	-28.03		-37.29	-33.91	
1714397	6040058	OTAIKA-5	OA157-54	Otakaranga at confluence	1.71	-25.85	-33.23	-32.62	-37.24	
1712330	6037916	OTAIKA-6	OA157-55	Otakaranga at top	2.10	-27.17	-32.73	-28.51	-28.05	-22.49
1712636	6040525	OTAIKA-7	OA157-56	Otaika (above Otakaranga Confluence)	2.80	-27.39		-31.15	-23.29	
1717641	6038763	PUWERA-1	OA157-69	Puwera (above confluence with Otaika)	2.94	-26.59	-29.33	-27.84	-28.13	
1720060	6051319	HA-1	OA157-57	Hatea Upper River (Waitaua branch)	2.44	-26.10				
1720556	6051935	HA-2	OA157-58	Hatea Upper River (Mangakino branch)	4.94	-27.54	-34.88	-30.79	-30.70	-30.65
1720823	6050317	HA-3	OA157-61	River bed sediment (Whangarei Falls)	2.14	-26.39		-31.46	-33.06	
1720953	6049026	HA-4	OA157-62	River bed sediment (Otangarei)	0.99	-24.35	-20.48	-20.47		
1720311	6047159	HA-5	OA157-63	River bed sediment (Mair Park)	2.15	-26.78	-34.81	-31.11	-30.24	-29.03
1717284	6044245	RAU-6	OA157-66	Raumanga (above confluence with Waiarohia)	0.54	-25.78				
1719086	6045695	WA-1	OA157-76	Raumanga (below confluence with Waiarohia)	0.58	-25.52		-30.75		
1720238	6044102	LBC-1	OA157-80	Limeburners Creek	1.57	-25.12	-25.71	-28.09		-28.92
1721645	6044975	KPC-1	OA157-74	Waioneone Creek (Kissing Point Creek)	3.42	-24.43	-33.68	-31.95	-30.62	-36.59
1723601	6044828	AWA-1R	OA157-75	Awaroa Creek	1.75	-26.09		-37.15		
1726447	6040757	WKK-1	OA157-67	Waikaraka Stream	0.21	-24.66		-20.33		
1724700	6042174	WKK-2	OA157-68	Waikaraka Stream	3.70	-25.00	-30.31	-27.68	-26.39	-25.75
1729226	6039405	PAU-3	OA157-71	Paura Bay	1.64	-25.62	-28.77	-28.26	-36.93	-30.83
1735930	6035459	McG-3	OA157-73	McGregors Creek	0.32	-25.40		-25.02		
1733445	6033069	BS-1	OA157-77	Black Smith Creek	0.35	-15.52	-20.93	-18.76	-21.96	-18.76
1728505	6033041	TK-1	OA157-78	Takahiwai Creek	0.25	-23.87	-30.46	-26.19		
1734331	6038769	MUNRO	OA157-79	Munro Bay	5.95	-24.40	-27.90	-27.97	-20.24	-22.67
1720717	6051970	HA-2a	OA157-59	Steep Pasture	6.06	-25.62	-39.14	-33.68	-30.15	
1720717	6051970	HA-2b	OA157-60	Flat eroded pasture	6.27	-24.85	-31.08	-25.54	-26.69	
1719865	6035262	PASTURE-1	OA157-81	Dairy Pasture ( Generic)	6.55	-25.27		-24.21	-31.00	-24.43
1715846	6039859	NATIVE	OA157-84	Native (Generic)	22.33	-27.00	-35.04	-30.66	-27.57	-25.37
1721020	6048921	OTAIKA-2 NF	OA157-83	Flood plain native forest (north-east side of Otaika)	7.77	-28.18	-38.30	-32.45	-36.11	-33.77
1720155	6034977	TOTARA	OA157-82	Totara (Generic)	9.69	-27.53		-31.15	-32.23	-31.52
1712804	6038478	RBET	OA157-70	Bank erosion Travinor Rd	0.33	-24.86		-24.20		
1717108	6043754	RAU-B1	OA157-64	Bank erosion (Raumanga Slipface)	2.30	-26.88	-30.54	-27.75	-26.74	

<b>Easting (NZMG)</b>	<b>Northing (NZMG)</b>	<b>Site Code</b>	<b>Sample ID</b>	<b>Sample Description</b>	<b>Carbon (%)</b>	<b>delta c13/C12</b>	<b>c14:0</b>	<b>c16:0</b>	<b>c18:0</b>	<b>c18:1 w9c</b>
1717225	6044103	RAU-3	OA157-65	Bank erosion (Maunu Rd)	0.43	-24.21		-30.04		
1725671	6044381	Forest regrowth 384	OA157-85	Pine forestry	0.51	-25.18				
1725854	6044267	Forest recent fell 385	OA157-86	Pine forestry	1.86	-25.81				
1725338	6044021	Forest Mature 386	OA157-87	Pine forestry	9.04	-26.64	-38.33	-30.73	-28.65	
1728412	6045010	Forest Rd cut face 383	OA157-88	Pine forestry	0.07	-25.44				
1718850	6036640	Portland Quarry	OA157-89	Quarry sand	0.60	-26.69				

## Harbour sample locations

Easting (NZMG)	Northing (NZMG)	Site Code	Sample ID	Sampling method	Carbon (%)	delta C <sup>13</sup> C <sup>12</sup>	c14:0	c16:0	c18:0	c18:1w9c
1721844	6041200	WHG-1	OA157-1	Helicopter	0.60	-9.11	-22.55	-19.58	-20.72	-17.79
1720826	6041978	WHG-2	OA157-2	Helicopter	1.40	-22.59	-23.92	-22.02	-25.61	-29.56
1720418	6040450	WHG-3	OA157-3	Helicopter	0.39	-21.48	-24.93	-24.99	-25.10	-27.15
1720695	6038918	WHG-4	OA157-4	Helicopter	0.18	-19.67	-21.09	-17.56	-18.36	-23.36
1721198	6038510	WHG-5	OA157-5	Helicopter	2.34	-6.57	-23.46	-20.03	-21.31	-24.23
1721674	6037706	WHG-6	OA157-6	Helicopter	0.50	-20.01	-25.98	-20.93	-21.65	-20.91
1721453	6035852	WHG-7	OA157-7	Helicopter	1.16	-17.01	-22.00	-20.44	-23.06	-22.89
1720532	6035737	WHG-8	OA157-8	Helicopter	0.72	-20.67	-21.74	-19.52		
1721624	6035212	WHG-9	OA157-9	Helicopter	0.93	-23.43	-23.37	-23.57	-20.34	-19.70
1720859	6034518	WHG-10	OA157-10	Helicopter	1.25	-22.91	-29.47	-25.42	-24.85	-25.46
1722263	6034611	WHG-11	OA157-11	Helicopter	1.55	-20.38	-25.13	-21.40	-24.11	-23.81
1722448	6035496	WHG-12	OA157-12	Helicopter	1.42	-21.68	-23.97	-24.41	-26.15	-25.98
1722556	6036358	WHG-13	OA157-13	Helicopter	0.37	-17.55	-20.56	-19.99	-24.13	-24.47
1722311	6037087	WHG-14	OA157-14	Helicopter	0.15	-17.20	-23.15	-24.23	-27.90	-25.39
1722532	6037784	WHG-15	OA157-15	Helicopter	0.11	-17.59	-21.26	-19.51	-17.48	-21.86
1722471	6038724	WHG-16	OA157-16	Helicopter	0.14	-19.17	-19.78	-17.13	-21.56	-22.52
1723996	6039435	WHG-17	OA157-17	Helicopter	0.12	-17.65	-21.36	-13.64	-10.00	-9.93
1724155	6038684	WHG-18	OA157-18	Helicopter	0.15	-16.29	-19.25	-16.16	-17.14	-18.52
1724805	6038196	WHG-19	OA157-19	Helicopter	0.08	-19.54	-24.05	-21.26	-21.73	-22.51
1724824	6037219	WHG-20	OA157-20	Helicopter	0.12	-18.57	-26.35	-20.12		-24.07
1723927	6036072	WHG-21	OA157-21	Helicopter	0.17	-17.65	-26.62	-18.51	-22.77	-21.17
1724840	6035909	WHG-22	OA157-22	Helicopter	0.32	-19.47	-24.00	-19.56	-24.23	-25.31
1726203	6036361	WHG-23	OA157-23	Helicopter	0.74	-16.95	-20.28	-16.22	-19.23	-22.23
1726868	6035682	WHG-24	OA157-24	Helicopter	0.75	-18.99	-25.46	-22.33	-25.05	-26.66
1727603	6035088	WHG-25	OA157-25	Helicopter	0.37	-18.94	-20.18	-17.99	-19.70	-23.75
1728335	6039105	WHG-26	OA157-26	Helicopter	0.26	-19.60	-20.29	-17.48		-12.74
1727755	6039468	WHG-27	OA157-27	Helicopter	0.12	-19.88		-18.13		
1727781	6038653	WHG-28	OA157-28	Helicopter	0.17	-19.06	-23.81	-22.82	-23.79	-23.99
1726467	6040204	WHG-29	OA157-29	Helicopter	0.45	-23.00	-30.19	-21.94		
1725823	6041077	WHG-30	OA157-30	Helicopter	0.93	-21.72	-19.26	-19.17		-24.46
1724058	6040819	WHG-31	OA157-31	Helicopter	0.68	-21.22	-29.33	-26.58	-34.57	-33.11
1721851	6040298	WHG-32	OA157-32	Helicopter	0.22	-17.93	-21.46	-17.93	-20.71	-20.41
1722550	6042003	WHG-33	OA157-33	By land	1.09	-22.54	-26.66	-25.91	-29.16	-30.33
1722598	6041641	WHG-34	OA157-34	By land	0.15	-20.67	-24.68	-21.30	-23.47	-22.87
1722652	6041158	WHG-35	OA157-35	By land	0.16	-19.84	-23.89	-21.01	-25.71	-25.10
1721480	6034400	WHG-1 CORE	OA157-36	Cores from boat	1.47	-17.70	-29.24	-28.39	-32.00	-29.55
1721300	6036120	WHG-2 CORE	OA157-37	Cores from boat	1.67	-9.73	-29.47	-23.49	-22.79	-25.13
1722400	6037540	WHG-3 CORE	OA157-38	Cores from boat	0.53	-17.94	-23.33	-22.70	-26.30	
1721260	6039160	WHG-4 CORE	OA157-39	Cores from boat	0.24	-19.45	-21.96	-18.19		
1721304	6039940	WHG-5 CORE	OA157-40	Cores from boat	0.06	-16.64	-23.23	-20.50		-22.27

<b>Easting (NZMG)</b>	<b>Northing (NZMG)</b>	<b>Site Code</b>	<b>Sample ID</b>	<b>Sampling method</b>	<b>Carbon (%)</b>	<b>delta c<sup>13</sup>/C<sup>12</sup></b>	<b>c14:0</b>	<b>c16:0</b>	<b>c18:0</b>	<b>c18: 1w9c</b>
1721160	6041420	WHG-6 CORE	OA157-41	Cores from boat	0.98	-23.23	-24.30	-23.62	-27.76	-22.51
1734360	6038520	WHG-7 CORE	OA157-42	Cores from boat	0.62	-20.97	-23.10	-19.49	-18.15	-23.16
1730025	6034750	WHG-8 CORE	OA157-43	Cores from boat	0.21	-17.06	-27.12	-25.64	-25.28	-20.66
1731360	6038240	WHG-9 CORE	OA157-44	Cores from boat	0.08	-18.41	-16.95	-15.80		-12.88
1731880	6039770	WHG-10 CORE	OA157-45	Cores from boat	0.70	-21.90	-25.78	-23.88		
1730160	6039120	WHG-11 CORE	OA157-46	Cores from boat	0.24	-20.35	-25.42	-18.93	-25.71	-21.15
1733390	6033500	WHG-12 CORE	OA157-47	Cores from boat	0.68	-20.26	-27.88	-20.01	-28.55	-24.65
1730800	6038970	WHG-13 CORE	OA157-48	Cores from boat	0.95	-21.65	-21.13	-20.17		-21.51
1733453	6033425	BB1 CORE	OA157-49	Cores from boat	0.01	-20.69	-25.35	-20.28		-26.23
1737160	6033360	CALLIOPE BAY CORE	OA157-50	Cores from boat	0.08	-17.76	-24.16	-19.05	-31.01	-18.73

## Appendix C Radioisotope dating

Radioisotopes, such as caesium-137 ( $^{137}\text{Cs}$ ,  $\frac{1}{2}$ -life 30 years) and lead-210 ( $^{210}\text{Pb}$ ,  $\frac{1}{2}$ -life 22.3 years), and plant pollen can be used to reconstruct the recent sedimentation history of an estuary.

Dating of estuarine sediments using independent methods offsets the limitations of any one approach. This is particularly important when interpreting sediment profiles from lakes and estuaries, given the confounding effects of physical and biological mixing (Robbins and Edgington, 1975; Sharma et al. 1987; Alexander et al. 1993; Valette-Silver, 1993; Benoit et al. 1999). A description of the various methods of dating sediments follows.

The S.I. unit of radioactivity used in this study is the Becquerel (Bq), which is equivalent to one radioactive disintegration per second.

### $^{137}\text{Cs}$ dating

$^{137}\text{Cs}$  was introduced to the environment by atmospheric nuclear weapons tests in 1953, 1955–1956 and 1963–1964. Peaks in annual  $^{137}\text{Cs}$  deposition corresponding to these dates are the usual basis for dating sediments (Wise, 1977; Ritchie and McHenry, 1989). Although direct atmospheric deposition of  $^{137}\text{Cs}$  into estuaries is likely to have occurred,  $^{137}\text{Cs}$  is also incorporated into catchment soils, which are subsequently eroded and deposited in estuaries (Figure C-1). In New Zealand,  $^{137}\text{Cs}$  deposition was first detected in 1953 and its annual deposition was been measured at several locations until 1985. Annual  $^{137}\text{Cs}$  deposition can be estimated from rainfall using known linear relationships between rainfall and Strontium-90 ( $^{90}\text{Sr}$ ) and measured  $^{137}\text{Cs}/^{90}\text{Sr}$  deposition ratios (Matthews, 1989). Experience in Auckland estuaries shows that  $^{137}\text{Cs}$  profiles measured in estuarine sediments bear no relation to the record of annual  $^{137}\text{Cs}$  deposition (i.e., 1955–1956 and 1963–1964  $^{137}\text{Cs}$ -deposition peaks absent), but rather preserve a record of direct and indirect (i.e., soil erosion) atmospheric deposition since 1953 (Swales et al. 2002). The maximum depth of  $^{137}\text{Cs}$  occurrence in sediment cores (corrected for sediment mixing) is taken to coincide with the year 1953, when  $^{137}\text{Cs}$  deposition was first detected in New Zealand. We assume that there is a negligible delay in initial atmospheric deposition of  $^{137}\text{Cs}$  in estuarine sediments (e.g.,  $^{137}\text{Cs}$  scavenging by suspended particles) whereas there is likely to have been a time-lag (i.e., <1 yr) in  $^{137}\text{Cs}$  inputs to estuaries from topsoil erosion, which would coincide with the occurrence of floods.

If a surface mixed layer (SML) is evident in a core, as shown by an x-ray image and/or a tracer profile (e.g.,  $^7\text{Be}$ ,  $^{210}\text{Pb}$ ) then  $^{137}\text{Cs}$  is likely to have been rapidly mixed through the SML. Therefore, to calculate time-averaged sedimentation rates, the maximum depth of  $^{137}\text{Cs}$  occurrence is reduced by the maximum depth of the SML.

Uncertainty in the maximum depth of  $^{137}\text{Cs}$  results from: (1) the depth interval between sediment samples and (2) minimum detectable concentration of  $^{137}\text{Cs}$ , which is primarily determined by sample size and counting time. The 1963–1964  $^{137}\text{Cs}$  deposition peak was about five-times than the deposition plateau that occurred between 1953 and 1972. Thus, depending on the sample size, there is uncertainty in the age of the maximum  $^{137}\text{Cs}$  depth (i.e., 1953–1963). To reduce this uncertainty, we have maximised the sample mass that is analysed.

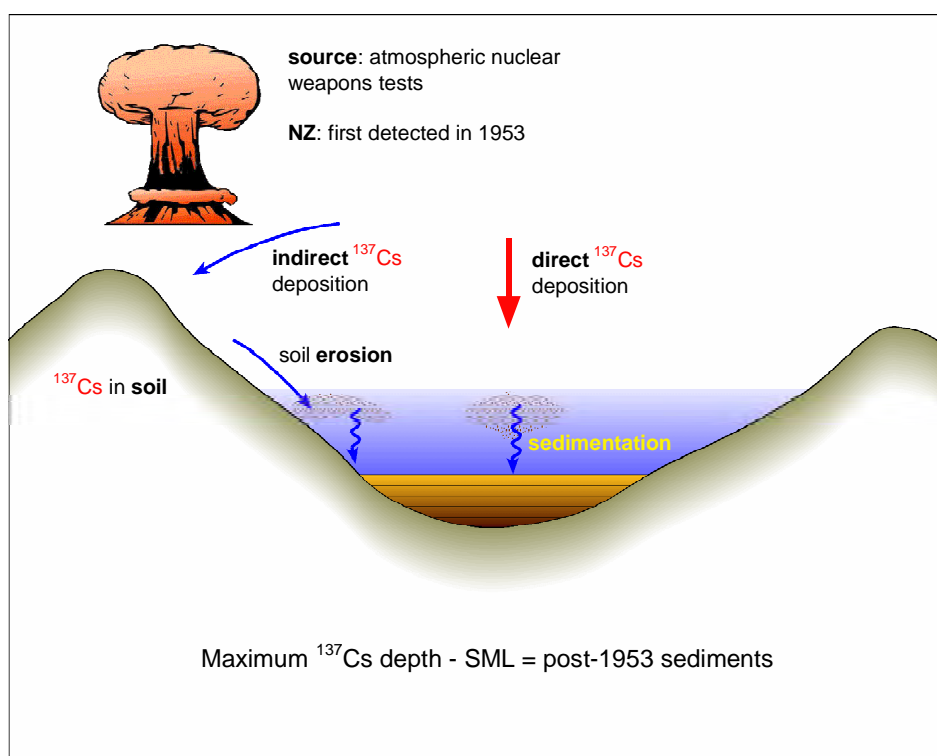


Figure C-1:  $^{137}\text{Cs}$  pathways to estuarine sediments.

### $^{210}\text{Pb}$ dating

$^{210}\text{Pb}$  (half-life 22.3 yr) is a naturally occurring radioisotope that has been widely applied to dating recent sedimentation (i.e., last 150 yrs) in lakes, estuaries and the sea (Figure C-2).  $^{210}\text{Pb}$  is an intermediate decay product in the uranium-238 ( $^{238}\text{U}$ ) decay series and has a radioactive decay constant ( $k$ ) of  $0.03114 \text{ yr}^{-1}$ . The intermediate parent radioisotope radium-226 ( $^{226}\text{Ra}$ , half-life 1622 years) yields the inert gas radon-222 ( $^{222}\text{Rn}$ , half-life 3.83 days), which decays through several short-lived radioisotopes to produce  $^{210}\text{Pb}$ . A proportion of the  $^{222}\text{Rn}$  gas formed by  $^{226}\text{Ra}$  decay in catchment soils diffuses into the atmosphere where it decays to form  $^{210}\text{Pb}$ . This atmospheric  $^{210}\text{Pb}$  is deposited at the earth surface by dry deposition or rainfall. The  $^{210}\text{Pb}$  in estuarine sediments has two components: supported  $^{210}\text{Pb}$  derived from *in situ*  $^{222}\text{Rn}$  decay (i.e., within the sediment column) and an unsupported  $^{210}\text{Pb}$  component derived from atmospheric fallout. This unsupported  $^{210}\text{Pb}$  component of the total  $^{210}\text{Pb}$  concentration in excess of the supported  $^{210}\text{Pb}$  value is estimated from the  $^{226}\text{Ra}$  assay (see below). Some of this atmospheric unsupported  $^{210}\text{Pb}$  component is also incorporated into catchment soils and is subsequently eroded and deposited in estuaries. Both the direct and indirect (i.e., soil inputs) atmospheric  $^{210}\text{Pb}$  input to receiving environments, such as estuaries, is termed the unsupported or excess  $^{210}\text{Pb}$ .

The concentration profile of unsupported  $^{210}\text{Pb}$  in sediments is the basis for  $^{210}\text{Pb}$  dating. In the absence of atmospheric (unsupported)  $^{210}\text{Pb}$  fallout, the  $^{226}\text{Ra}$  and  $^{210}\text{Pb}$  in estuary sediments would be in radioactive equilibrium, which results from the substantially longer  $^{226}\text{Ra}$  half-life. Thus, the  $^{210}\text{Pb}$  concentration profile would be uniform with depth. However, what is typically observed is a reduction in  $^{210}\text{Pb}$  concentration with depth in the sediment

column. This is due to the addition of unsupported  $^{210}\text{Pb}$  directly or indirectly from the atmosphere that is deposited with sediment particles on the bed. This unsupported  $^{210}\text{Pb}$  component decays with age ( $k = 0.03114 \text{ yr}^{-1}$ ) as it is buried through sedimentation. In the absence of sediment mixing, the unsupported  $^{210}\text{Pb}$  concentration decays exponentially with depth and time in the sediment column. The validity of  $^{210}\text{Pb}$  dating rests on how accurately the  $^{210}\text{Pb}$  delivery processes to the estuary are modelled, and in particular the rates of  $^{210}\text{Pb}$  and sediment inputs (i.e., constant versus time variable)

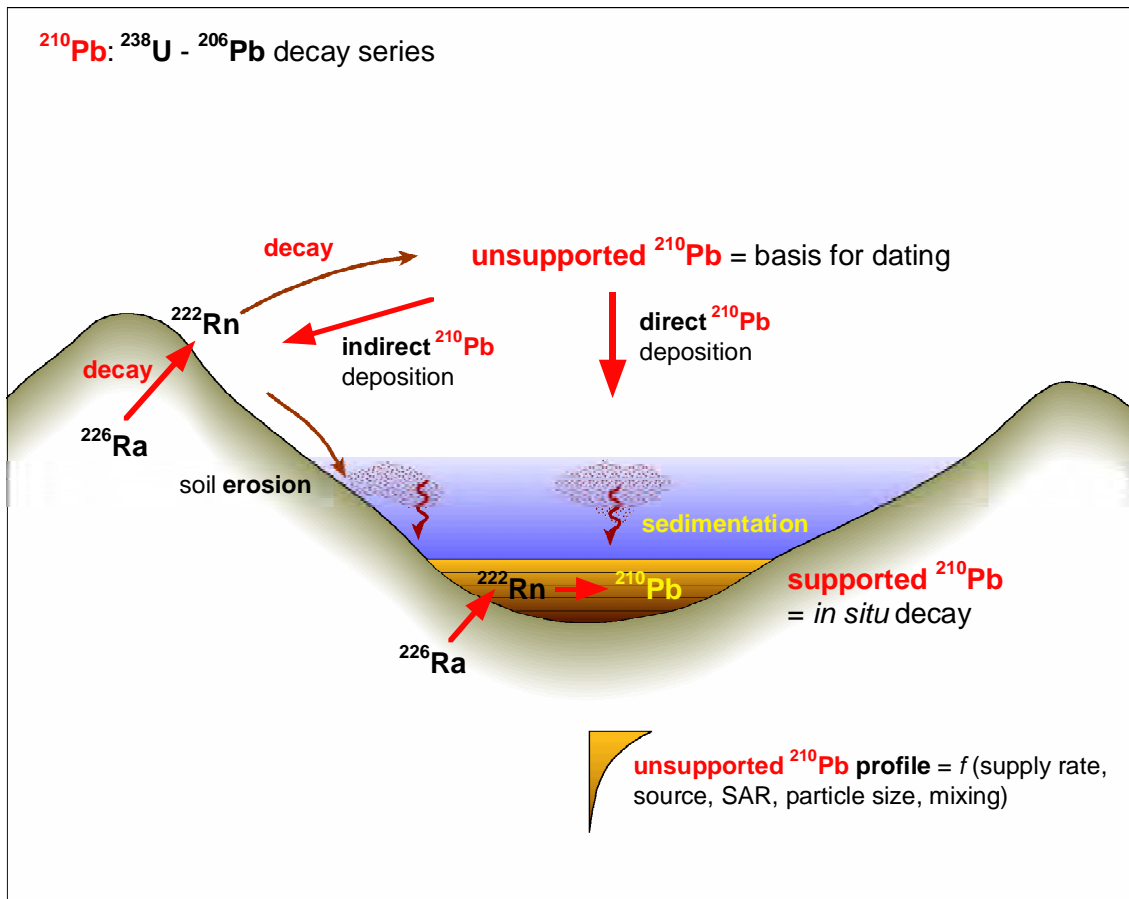


Figure C-2:  $^{210}\text{Pb}$  pathways to estuarine sediments.

### Sediment accumulation rates (SAR)

Sedimentation rates calculated from cores are **net average sediment accumulation rates (SAR), which are usually expressed as  $\text{mm yr}^{-1}$** . These SAR are net values because cores integrate the effects of all processes, which influence sedimentation at a given location. At short time scales (i.e., seconds–months), sediment may be deposited and then subsequently resuspended by tidal currents and/or waves. Thus, over the long term, sedimentation rates derived from cores represent net or cumulative effect of potentially many cycles of sediment deposition and resuspension. However, less disrupted sedimentation histories are found in depositional environments where sediment mixing due to physical processes (e.g., resuspension) and bioturbation is limited. The effects of bioturbation on sediment profiles and dating resolution reduce as SAR increase (Valette-Silver, 1993).

Net sedimentation rates also mask the fact that sedimentation is an episodic process, which largely occurs during catchment floods, rather than the continuous gradual process that is implied. In large estuarine embayments, such as the Firth, mudflat sedimentation is also driven by wave-driven resuspension events. Sediment eroded from the mudflat is subsequently re-deposited elsewhere in the estuary.

Although sedimentation rates are usually expressed as a sediment thickness deposited per unit time (i.e., mm yr<sup>-1</sup>) this statistic does not account for changes in dry sediment mass with depth in the sediment column due to compaction. Typically, sediment density ( $\rho = \text{g cm}^{-3}$ ) increases with depth and therefore some workers prefer to calculate dry mass accumulation rates per unit area per unit time ( $\text{g cm}^{-2} \text{yr}^{-1}$ ). These data can be used to estimate the total mass of sedimentation in an estuary (tonnes yr<sup>-1</sup>) (e.g., Swales et al. 1997). However, the effects of compaction can be offset by changes in bulk sediment density reflecting layering of low-density mud and higher-density sand deposits. Furthermore, the significance of a SAR expressed as mm yr<sup>-1</sup> is more readily grasped than a dry-mass sedimentation rate in  $\text{g cm}^{-3} \text{yr}^{-1}$ . For example, the rate of estuary aging due to sedimentation (mm yr<sup>-1</sup>) can be directly compared with the local rate of sea level rise.

The equations used to estimate time-averaged SAR from the excess <sup>210</sup>Pb and <sup>137</sup>Cs profiles are described below.

### Estimating SAR using <sup>210</sup>Pb profiles

The rate of decrease in excess <sup>210</sup>Pb activity with depth can be used to calculate a net sediment accumulation rate. The excess <sup>210</sup>Pb activity at time zero ( $C_0$ , Bq kg<sup>-2</sup>), declines exponentially with age ( $t$ ):

$$C_t = C_0 e^{-kt}$$

Assuming that within a finite time period, sedimentation ( $S$ ) is constant then  $t = z/S$  can be substituted into the above equation and by re-arrangement:

$$\frac{\ln \left[ \frac{C_t}{C_0} \right]}{z} = -k / S$$

Because excess <sup>210</sup>Pb<sub>us</sub> activity decays exponentially and assuming that sediment age increases with depth, a vertical profile of natural log( $C$ ) should yield a straight line of slope  $b = -k/S$ . A linear regression model is fitted to natural-log transformed excess <sup>210</sup>Pb data to calculate  $b$ . The SAR over the depth of the fitted data is given by:

$$S = -(k) / b$$

An advantage of the <sup>210</sup>Pb-dating method is that the SAR is based on the excess <sup>210</sup>Pb profile rather than a single layer or horizon, as is the case for <sup>137</sup>Cs where the maximum penetration depth of this radioisotope is used for dating. Furthermore, if the <sup>137</sup>Cs tracer is present at the bottom of the core then the estimated SAR represents a minimum value.

### Estimating SAR using $^{137}\text{Cs}$ profiles

The  $^{137}\text{Cs}$  profiles will also be used to estimate time-averaged SAR based on the maximum depth of  $^{137}\text{Cs}$  in the sediment column, corrected for surface mixing. The  $^{137}\text{Cs}$  SAR is calculated as:

$$S = (M - L) / T - T_0$$

where  $S$  is the  $^{137}\text{Cs}$  SAR,  $M$  is the maximum depth of the  $^{137}\text{Cs}$  profile,  $L$  is the depth of the surface mixed layer (SML) indicated by the  $^7\text{Be}$  profile and/or x-ray images,  $T$  is the year cores were collected and  $T_0$  is the year (1953)  $^{137}\text{Cs}$  deposition was first detected in New Zealand.

### Sediment mixing

Biological and physical processes, such as the burrowing and feeding activities of animals and/or sediment resuspension by waves (Figure C-3), mix the upper sediment column (Bromley, 1996). As a result, sediment profiles are modified and this limits the temporal resolution of dating. Various mathematical models have been proposed to take into account the effects of bioturbation on  $^{210}\text{Pb}$  concentration profiles (e.g., Guinasso and Schink, 1975).

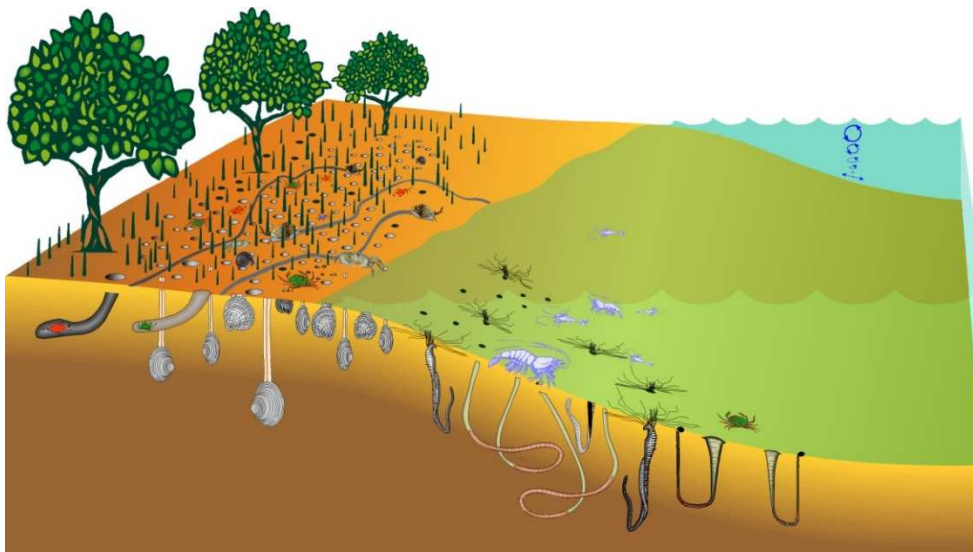


**Figure C-3: Biological and physical processes** such as the burrowing and feeding activities of animals and/or sediment resuspension by waves, mix the upper sediment column. As a result, sediment profiles are modified and limit the temporal resolution of dating. The surface mixed layer (SML) is the yellow zone.

Biological mixing has been modelled as a one-dimensional particle-diffusion process (Goldberg and Koide, 1962) and this approach is based on the assumption that the sum effect of 'random' biological mixing is integrated over time. In estuarine sediments exposed to bioturbation, the depth profile of unsupported  $^{210}\text{Pb}$  typically shows a two-layer form, with a surface layer of relatively constant unsupported  $^{210}\text{Pb}$  concentration overlying a zone of exponential decrease. In applying these types of models, the assumption is made that the mixing rate (i.e., diffusion co-efficient) and mixing depth (i.e., surface-mixed layer, SML) are uniform in time. The validity of this assumption usually cannot be tested, but changes in bioturbation process could be expected to follow changes in benthic community composition.

## Appendix D Compound specific stable isotopes

### Introduction to stable isotopes

In this section we describe how stable isotopes are used to identify the sources of catchment sediments deposited in lakes, estuaries and coastal waters and explain how isotopic data are interpreted.

Stable isotopes are non-radioactive and are a natural phenomenon in many elements. In the NIWA Compound Specific Stable Isotope (CSSI) method, carbon (C) stable isotopes are used to determine the provenance of sediments (Gibbs 2008). About 98.9% of all carbon atoms have an atomic weight (mass) of 12. The remaining ~1.1% of C atoms have an extra neutron in the atomic structure, giving it an atomic weight (mass) of 13. These are the two stable isotopes of carbon. Naturally occurring carbon also contains an extremely small fraction (about two trillionths) of radioactive carbon-14 ( $^{14}\text{C}$ ). Radiocarbon dating is also used in the present study to determine long-term sedimentation rates.

To distinguish between the two stable isotopes of carbon, they are referred to as light ( $^{12}\text{C}$ ) and heavy ( $^{13}\text{C}$ ) isotopes. Both of these stable isotopes of carbon have the same chemical properties and react in the same way. However, because  $^{13}\text{C}$  has the extra neutron in its atom, it is slightly larger than the  $^{12}\text{C}$  atom. This causes molecules with the  $^{13}\text{C}$  atoms in their structure to react slightly slower than those with  $^{12}\text{C}$  atoms, and to pass through cell walls in plants or animals at a slower rate than molecules with  $^{12}\text{C}$  atoms. Consequently, more of the  $^{12}\text{C}$  isotope passes through the cell wall than the  $^{13}\text{C}$  isotope, which results in more  $^{12}\text{C}$  on one side of the cell wall than the other. This effect is called isotopic fractionation and the difference can be measured using a mass spectrometer. Because the fractionation due to passage through one cell-wall step is constant, the amount of fractionation can be used to determine chemical and biological pathways and processes in an ecosystem. Each cell wall transfer or “step” is positive and results in enrichment of the  $^{13}\text{C}$  content.

The amount of fractionation is very small (about one thousandth of a percent of the total molecules for each step) and the numbers become very cumbersome to use. A convention has been developed where the difference in mass is reported as a ratio of heavy-to-light isotope. This ratio is called “delta notation” and uses the symbol “ $\delta$ ” before the heavy isotope symbol to indicate the ratio i.e.,  $\delta^{13}\text{C}$ . The units are expressed as “per mil” which uses the symbol “‰”. The delta value of a sample is calculated using the equation:

$$\delta^{13}\text{C} = \left[ \left( \frac{R_{\text{sample}}}{R_{\text{standard}}} \right) - 1 \right] 1000$$

where  $R$  is the molar ratio of the heavy to light isotope  $^{13}\text{C}/^{12}\text{C}$ . The international reference standard for carbon was a limestone, Pee Dee Belemnite (PDB), which has a  $^{13}\text{C}/^{12}\text{C}$  ratio of 0.0112372 and a  $\delta^{13}\text{C}$  value of 0 ‰. As all of this primary standard has been consumed, secondary standards calibrated to the PDB standard are used. Relative to this standard most organic materials have a negative  $\delta^{13}\text{C}$  value.

Atmospheric  $\text{CO}_2$ , which is taken up by plants in the process of photosynthesis, presently has a  $\delta^{13}\text{C}$  value of about -8.5. In turn, the  $\delta^{13}\text{C}$  signatures of organic compounds produced by plants partly depends on their photosynthetic pathway, primarily either  $\text{C}_3$  or  $\text{C}_4$ . During photosynthesis, carbon passes through a series of reactions or trophic steps along the  $\text{C}_3$  or

C<sub>4</sub> pathways. At each trophic step, isotopic fractionation occurs and organic matter in the plant (i.e., the destination pool) is depleted by 1 ‰. The C<sub>3</sub> pathway is longer than the C<sub>4</sub> pathway so that organic compounds produced by C<sub>3</sub> plants have a more depleted δ<sup>13</sup>C signature. There is also variation in the actual amount of fractionation between plant species having the same photosynthetic pathway. This results in a range of δ<sup>13</sup>C values, although typical bulk values for C<sub>3</sub> and C<sub>4</sub> plants vary around -26 ‰ and -12 ‰ respectively. The rate of fractionation also varies between the various types of organic compounds produced by plants. Thus, by these processes a range of organic compounds each with unique δ<sup>13</sup>C signatures are produced by plants that can potentially be used as natural tracers or biomarkers.

The instruments used to measure stable isotopes are called “isotope ratio mass spectrometers” (IRMS) and they report delta values directly. However, because they have to measure the amount of <sup>12</sup>C in the sample, and the bulk of the sample C will be <sup>12</sup>C, the instrument also gives the percent C (%C) in the sample.

When analysing the stable isotopes in a sample, the δ<sup>13</sup>C value obtained is referred to as the bulk δ<sup>13</sup>C value. This value indicates the type of organic material in the sample and the level of biological processing that has occurred. (Biological processing requires passage through a cell wall, such as in digestion and excretion processes and bacterial decomposition.) The bulk δ<sup>13</sup>C value can be used as an indicator of the likely source land cover of the sediment. For example, fresh soil from forests has a high organic content with %C in the range 5% to 20% and a low bulk δ<sup>13</sup>C value in the range -28‰ to -40‰. As biological processing occurs, bacterial decomposition converts some of the organic carbon to carbon dioxide (CO<sub>2</sub>) gas which is lost to the atmosphere. This reduces the %C value and, because microbial decomposition has many steps, the bulk δ<sup>13</sup>C value increases by ~1‰ for each step. Pasture land cover and marine sediments typically have bulk δ<sup>13</sup>C values in the range -24‰ to -26‰ and -20‰ to -22‰, respectively. Waste water and dairy farm effluent have bulk δ<sup>13</sup>C values more enriched than -20‰. Consequently, a dairy farm where animal waste has been spread on the ground as fertilizer, will have bulk δ<sup>13</sup>C values higher (more enriched) than pasture used for sheep and beef grazing.

In addition to the bulk δ<sup>13</sup>C value, organic carbon compounds in the sediment can be extracted and the δ<sup>13</sup>C values of the carbon in each different compound can be measured. These values are referred to as compound-specific stable isotope (CSSI) values. A forensic technique recently developed to determine the provenance of sediment uses both bulk δ<sup>13</sup>C values and CSSI values from each sediment sample in a deposit for comparison with signatures from a range of potential soil sources for different land cover types. This method is called the CSSI technique (Gibbs, 2008).

The CSSI technique is based on the concepts that:

1. land cover is primarily defined by the plant community growing on the land, and
2. all plants produce the same range of organic compounds but with slightly different CSSI values because of differences in the way each plant species grows and also because each land cover type has a characteristic composition of plant types that contribute to the CSSI signature.

The compounds commonly used for CSSI analysis of sediment sources are natural plant fatty acids which bind to the soil particles as labels called biomarkers. While the amount of a biomarker may decline over time, the CSSI value of the biomarker does not change. The CSSI values for the range of biomarkers in a soil provides positive identification of the source of the soil by land cover type.

The sediment at any location in an estuary or harbour can be derived from many sources including river inflows, coastal sediments and harbour sediment deposits that have been mobilised by tidal currents and wind-waves. The contribution of each sediment source to the sediment mixture at the sampling location will be different. To separate and apportion the contribution of each source to the sample, a mixing model is used. The CSSI technique uses the mixing model IsoSource (Phillips & Gregg 2003). The IsoSource mixing model is described in more detail in a following section.

While the information on stable isotopes above has focused on carbon, these descriptions also apply to nitrogen (N), which also has two stable isotopes,  $^{14}\text{N}$  and  $^{15}\text{N}$ . The bulk N content (%N) and bulk isotopic values of N,  $\delta^{15}\text{N}$ , also provide information on land cover in the catchment but, because the microbial processes of nitrification and denitrification can cause additional fractionation after the sediment has been deposited, bulk  $\delta^{15}\text{N}$  cannot be used to identify sediment sources. The fractionation step for N is around +3.5‰ with bulk  $\delta^{15}\text{N}$  values for forest soils in the range +2‰ to +5‰. Microbial decomposition processes result in bulk  $\delta^{15}\text{N}$  values in the range 6‰ to 12‰ while waste water and dairy effluent can produce bulk  $\delta^{15}\text{N}$  values up to 20‰. However, the use of synthetic fertilizers such as urea, which has  $\delta^{15}\text{N}$  values of -5‰, can result in bulk  $\delta^{15}\text{N}$  values <0‰.

## Analyses

An aliquot of each dry sediment sample was acidified with 1 N hydrochloric acid to remove inorganic carbonate before analysing for bulk organic C and N stable isotopes. About 50 mg of each acidified sample was combusted in a helium gas stream in a Fisons N1500 Elemental Analyser coupled via a ConFlo-II interface to a Thermo-Finnegan Continuous Flow Isotope Ratio Mass Spectrometer (CF-IRMS).

For  $\delta^{13}\text{C}$ , CF-IRMS measurements typically have a precision of  $\pm 0.1$  ‰ or better and the instrument also provides the proportion of organic C and N (%) in each sample.

Aliquots (20 to 40 g) of the non-acidified dry sediment were extracted with hot dichloromethane (100 °C) under high pressure (2000 psi) in a Dionex Accelerated Solvent Extractor (ASE 2000) to extract the fatty acids bound to the sediment particles. The fatty acids were methylated using 5% boron trifluoride catalyst in methanol to produce fatty acid methyl esters (FAMES). These FAMES were analysed by gas chromatography (GC)-combustion-IRMS to produce compound-specific stable isotope  $\delta^{13}\text{C}$  values i.e., CSSI values. Method details and data interpretation protocols were described previously by Gibbs (2008).

## Data processing and presentation

The bulk  $\delta^{13}\text{C}$  values, %C and suite of CSSI values for the extracted FAMES were assembled into a matrix table and modelled using IsoSource to estimate the number ( $n$ ) of isotopically feasible proportions of the main sediment sources at each sampling location. In

successive model iterations, potential sources were added or removed to find an isotopic balance where the confidence level was high (lowest  $n$  value) and uncertainty was low. The isotopically feasible proportions of each soil source are then converted to soil proportions using the %C of each soil on a proportional basis. That is to that the higher the %C in the soil, the less of that soil source is required to obtain the isotopic balance. In general, soil proportions less than 5% were considered possible but potentially not present. Soil proportions >5% were considered to be present within the range of the mean  $\pm$  SD.

The per cent-soil proportions for the major river inflows were then plotted as spatial distribution maps of the BOI system using the contouring programme “Surfer-V8” (Golden Software), using linear kriging. Because of the paucity of data, the contour plots produced by linear kriging are indicative rather than definitive.

### CSSI Method

The CSSI method applies the concept of using the  $\delta^{13}\text{C}$  signatures of organic compounds produced by plants to distinguish between soils that develop under different land-cover types. With the exception of monocultures (e.g., wheat field), the  $\delta^{13}\text{C}$  signatures of each land-cover type reflects the combined signatures of the major plant species that are present. For example, the isotopic signature of the Bay’s lowland native forest will be dominated by kauri, rimu, totara and tānekaha. A monoculture, such as pine forest, by comparison will impart an isotopic signature that largely reflects the pine species, as well as, potentially, any understory plants.

The application of the CSSI method for sediment-source determination involves the collection of sediment samples from potential sub-catchment and/or land cover sources as well as sampling of sediment deposits in the receiving environment. These sediment deposits are composed of mixtures of terrigenous sediments, with the contribution of each source potentially varying both temporally and spatially. The sampling of catchment soils provides a library of isotopic signatures of potential sources that is used to model the most likely sources of sediments deposited at any given location and/or time.

Straight-chain Fatty Acids (FA) with carbon-chain lengths of 12 to 24 atoms (C12:0 to C24:0) have been found to be particularly suitable for sediment-source determination as they are bound to fine sediment particles and long-lived (i.e., decades). In the present study, five types of FA were used to evaluate the present-day and historical sources of terrigenous sediments deposited in the Bay: Myristic Acid (C14:0); Palmitic (C16:0); Stearic (C18:0); Arachidic (C20:0) and Behenic (C22:0). Although breakdown of these FA to other compounds eventually occurs, the signature of a remaining FA in the mixture does not change.

The stable isotope compositions of N and C and the CSSI of carbon in the suite of fatty acid (FA) biomarkers are extracted from catchment soils and marine sediments. It is the FA signatures of the soils and marine sediments that are used in this study to determine sediment sources. Gibbs (2008) describes the CSSI method in detail.

## IsoSources mixing model

The sources of terrigenous sediments deposited on the present-day seabed surface and at various times in the past, that are preserved in cores, were determined from analysis of the CSSI signatures of potential sources (i.e., soils) and mixtures (i.e., marine-sediment deposits). The library of isotopic signatures used included those derived from local (i.e., Bay of Islands) soils as well as other potential sources that were not sampled because (1) they could not be accessed or (2) no longer occur in the catchment (e.g., kumara gardens).

In the present study, the IsoSource mixing model (Phillips & Gregg 2003) was used to evaluate the feasible sources of terrigenous sediments in the estuarine deposits. IsoSource requires a minimum of three sources and two isotopic tracers to run. In the present study, an iterative approach was taken to the selection of potential sediment sources, constrained by the recorded land-cover history. For example, in the Bay of Island's, citrus trees were not planted in large numbers in the Kerikeri catchment until the late 1920s so that citrus is not a valid sediment source for sediments deposited before that time.

IsoSource is not a conventional mixing model in that it iteratively constructs a table of all possible combinations of isotopic source proportions that sum to 100% and compares these predicted isotopic values with the isotopic values in the sediment mixture (i.e., deposit). If the predicted and observed stable isotope values are equal or within some small tolerance (e.g., 0.1 ‰, referred to as the mass-balance tolerance by Phillips and Gregg 2003) then that predicted stable-isotope signature represents a feasible solution. Within a given tolerance, there may be few or many feasible solutions.

The total number of feasible solutions ( $n$ ) provides a measure of the confidence in the result. High values of  $n$  indicate many feasible solutions and hence there is low confidence in the result. As the value of  $n$  reduces towards 1 the level of confidence increases until  $n = 1$ , which represents a unique solution. It is rare to have an exact match or unique solution. In most cases there will be many feasible solutions and these can be statistically evaluated to assess the most likely combination of sources in the sediment sample. These feasible solutions are expressed as isotopic feasible proportions (%) with an uncertainty value equivalent to the standard deviation about the mean.

In practice, the tolerance is reduced by iteration within the IsoSource model to obtain the lowest  $n$  and therefore the highest confidence in the result. The tolerance required to obtain any feasible solutions will be greater than 0.1 ‰ if the isotopic values of the source tracers differ markedly from those of the sediment mixture in the receiving environment. Together, the tolerance and number of feasible solutions ( $n$ ) for each sediment mixture provide measures of uncertainty in the results in addition to the standard deviation and the range of the isotopic proportions for each soil source. An example result from this analysis for a Bay of Islands sediment sample is shown in Table D-1 below (Swales et al. 2012).

**Table D-1: Example of IsoSource model result.** Core RAN-5B (Waikare Inlet), 30-31 cm depth (1914 AD). The mean, median and standard deviation (SD) values are shown.

Tolerance	n	Nikau			Kauri			Bracken		
		mean	median	SD	mean	median	SD	mean	median	SD
0.9	3	0.317	0.32	0.006	0.55	0.55	0.01	0.133	0.13	0.006

This sample comes from core RAN-5B, which was collected in the Waikare Inlet. The catchment even today remains largely under native forest and scrub land cover, so that sediments deposited in the inlet should reflect these land cover signatures. The sample was taken from 30—31-cm depth in the core, with radioisotope dating indicating that it was deposited in the early 1900s. The feasible isotopic proportions of the three major sediment sources are shown in the table (range = 0–1, where 1 = 100%). Although mean, median and standard deviation values are shown, minimum and maximum values of the feasible isotopic proportions for each source are also calculated. **The reporting solely of mean values is not adequate** and a measure of uncertainty, such as the minimum, maximum and/or standard deviation should be included in the results (Phillips & Gregg 2003).

The results indicate that the soils that make up the sediment-core sample are largely derived from native forest (kauri and nikau associations), with a small contribution from bracken. The presence of bracken is a key indicator of catchment disturbance/forest clearing. The presence of bracken pollen in sediment deposits has long been used in historical reconstructions of the New Zealand environment (e.g., McGlone 1983). However, bracken pollen reflects the presence of these plants growing in the general area and may or may not be indicative of bracken soils being eroded. By comparison, the presence of a CSSI bracken signature in a deposit positively indicates that some proportion of the sediment sample is composed of eroded bracken soil. The tolerance at 0.9 ‰ is a mid-range value, with values as low as 0.01 ‰ possible in some of the samples that were analysed. The number of feasible solutions ( $n = 3$ ) is low, which also provides high confidence in these results.

Typically less than 5% of most sediment samples is composed of carbon, and the isotopic balance evaluated by IsoSource is only applicable to the carbon content of each source. These isotopically feasible proportions must therefore be converted to soil proportions using a linear scaling factor to estimate the percent contribution of each feasible soil source. This conversion of feasible isotopic source proportions to soil source proportions is described in a following section.

### Conversion of isotopic proportions to soil proportions

The IsoSource model provides estimates of the isotopic-proportional contributions of each land-cover (i.e., soil) type in each marine sample. Thus, these results are in terms of carbon isotopic proportions and not source soil proportions. Furthermore, the stable isotope tracers account for a small fraction, typically less than 2%, of total organic carbon (OC) in the soil and OC accounts for typically <10% of the soil by weight. These factors mean that the contribution of each source soil to a sediment mixture will scale with the soil carbon content. Consequently, a linear correction based on the soil OC is required to estimate the proportion of each soil source in a sediment sample from a receiving environment (Gibbs 2008).

To convert the isotopic proportions to soil proportions ( $S_n\%$ ) the simple linear correction equation below was used:

$$S_n\% = \frac{I_n/C_n\%}{\sum_n^1 (I_n/C_n\%)} * 100$$

Where  $I_n$  is the mean feasible isotopic proportion of source soil  $n$  in the mixture estimated using an isotopic mixing model and  $C_n\%$  is the percentage organic carbon in the source soil.

Because this calculation only uses the OC% in the source soils for linear scaling, the proportional contribution of each source soil is not influenced by any loss of carbon (e.g., total carbon, Fatty Acids etc.,) in the sediment mixture due to biodegradation. The level of uncertainty in the mean soil proportion is the same as that defined by the standard deviation about the mean isotopic proportion.

A simple example of this linear correction is illustrated here by considering a solution composed of a mixture of three different sodium (Na) salts which provide equal proportions of Na to the mixture (3 x 1/3 each): sodium chloride (NaCl, molecular weight 58.45); sodium nitrate (NaNO<sub>3</sub>, mw 85.0); and sodium sulphate (Na<sub>2</sub>SO<sub>4</sub>, mw 142.0). Consider each of these salts to represent a different source soil, each of which are present in a sediment mixture. The %Na represents the % carbon in each source soil. The %Na in each salt is calculated by dividing the atomic weight of sodium (23) by the molecular weight of each salt compound.

Table D-2 below presents the calculations required to apply the linear correction equation using the sodium salts example in order to determine how much of each salt is in the mixture. The ratio M%/S% for each salt and sum of this ratio (4.14) represent the numerator and denominator respectively in the conversion equation. Thus, for example the proportion of NaCl salt in the mixture is given by  $(0.85/4.14)*100 = 20.5\%$ .

In the present study this linear conversion of isotopic proportions to soil source proportions was applied to the present-day surficial sediments. This correction process was not applied to the historical soil-source data from cores because %C data was not available for all soil sources. For example, although kumara and potato cultivation were important landuse types in some sub-catchments in the past, this is no longer the case. In this situation the isotopic signatures of the plants themselves and not the labelled soils were used in the isotope modelling.

**Table D-2: Example of the linear correction method** to convert the isotopic proportions to soil proportions using sodium (Na) salt compounds as analogies to various soil sources present in a mixture.

Salt type	%Na in salt (S%)	%Na in mixture (M%)	M%/S%	% salt in mixture
NaCl	39.4	33.3	0.85	20.5
NaNO <sub>3</sub>	27.1	33.3	1.23	29.8
Na <sub>2</sub> SO <sub>4</sub>	16.2	33.3	2.06	49.7
SUM			4.14	